Synthesis, Structure, Electrochemistry, and Spectroelectrochemistry of Hypervalent Phosphorus(V) Octaethylporphyrins and Theoretical Analysis of the Nature of the PO Bond in $P(OEP)(CH_2CH_3)(O)$

Kin-ya Akiba,*,† Ryo Nadano,† Wataru Satoh,† Yohsuke Yamamoto,*,† Shigeru Nagase,‡ Zhongping Ou,§ Xiaoyu Tan,§ and Karl M. Kadish*,§

Department of Chemistry, Graduate School of Science, Hiroshima University, 1-3-1 Kagamiyama, Higashi-Hiroshima 739-8526, Japan, Department of Chemistry, Graduate School of Science, Tokyo Metropolitan University, 1-1 Minami-osawa, Hachioji, Tokyo, 192-0397, Japan, and Department of Chemistry, University of Houston, Houston, Texas 77204-5641

Received June 5, 2001

A variety of phosphorus(V) octaethylporphyrin derivatives of the type $[P(OEP)(X)(Y)]^+Z^-$ (OEP: octaethylporphyrin) (X = CH_3, CH_2CH_3, C_6H_5, F; Y = CH_3, CH_2CH_3, OH, OCH_3, OCH_2CH_3, O*n*-Pr, O*i*-Pr, O*sec*-Bu, NHBu, NEt_2, Cl, F, O^-; Z = ClO_4, PF_6) were prepared. X-ray crystallographic analysis of eleven compounds reveals that the degree of ruffling of the porphyrin core becomes greater and the average P−N bond distance becomes shorter as the axial ligands become more electronegative. Therefore, the electronic effect of the axial substituents plays a major role in determining the degree of ruffling although the steric effect of the substituents plays some role. A comparison of the ^{1}H NMR chemical shifts for the series of $[P(OEP)(CH_2CH_3)(Y)]^+Z^-$ complexes with those of the corresponding arsenic porphyrins, which possess a planar core, indicates a much smaller ring current effect of the porphyrin core in the severely ruffled phosphorus porphyrins. The electrochemistry, spectroelectrochemistry and ESR spectroscopy of the singly reduced compounds are also discussed. The OH protons of $[P(OEP)(X)(OH)]^+$ are acidic enough to generate P(OEP)(X)(O) by treatment with aq dilute NaOH. X-ray analysis of $P(OEP)(CH_2CH_3)(O)$ reveals that the PO bond length is very short (1.475(7) Å) and is comparable to that in triphenylphosphine oxide (1.483 Å). The features of the quite unique hexacoordinate hypervalent compounds are investigated by density functional calculation of a model $(Por)P(CH_2CH_3)(O)$ and (Por)P(F)(O) (Por: unsubstituted porphyrin).

Introduction

Phosphorus is the smallest atom which can occupy the center of a porphyrin ring and a hexacoordination of the small phosphorus(V) ion was proposed to result in ruffling of the porphyrin macrocycle.[1] However, no systematic study as to the electronic effect of the axial ligands on the degree of ruffling of the porphyrin core has been carried out for phosphorus porphyrins although there have been several reports on the structures of phosphorus(V) tetraphenylporphyrin derivatives,[2−6] and on some unique properties of Group 15 element porphyrins such as the photoelectronic properties of Sb(III),[7] Sb(V),[8] and P(V) porphyrin oligomers,[9−15] redox electrochemistry,[16−20] and utilization as photochemical oxygenating reagents.[21−27]

* To whom correspondence should be sent.
† Hiroshima University.
‡ Tokoyo Metropolitan University.
§ University of Houston.

(1) (a) Hoard, J. L. *Science*, **1971**, *174*, 1295. (b) Hoard, J. L. *Porphyrins and Metalloporphyrins*; Smith, K. M., Ed.; Elsevier: Amsterdam, 1975; p317. (c) Kadish, K. M.; Smith, K. M.; Guilard, R. Ed., *The Porphyrin Handbook*; Academic Press: New York, 2000.
(2) Mangani, S.; Meyer, E. F.; Jr., Cullen, D. L.; Tsutsui, M.; Carrano, C. J. *Inorg. Chem.*, **1983**, *22*, 400.
(3) Lin, Y.-H.; Lin, C.-C.; Chen, J.-H.; Zeng, W.-F.; Wang, S.-S. *Polyhedron* **1994**, *13*, 2887.
(4) Lin, Y.-H.; Sheu, M.-T.; Lin, C.-C.; Chen, J.-H.; Wang, S.-S. *Polyhedron* **1994**, *13*, 3094.
(5) Guo, J. L.; Sun, F.; Li, Y.; Azuma, N. *Polyhedron* **1995**, *14*, 1471.
(6) Lin, Y.-H.; Tang, S.-S.; Lin, C.-C.; Chen, J.-H.; Zeng, W.-F.; Wang, S.-S.; Lin, H.-J. *Aust. J. Chem.* **1995**, *48*, 1367.
(7) Knör, G.; Vogler, A. *Inorg. Chem.* **1994**, *33*, 314.
(8) Kalyanasundaram, K.; Shelnutt, J. A.; Grätzel, M. *Inorg. Chem.* **1988**, *27*, 2820.
(9) Segawa, H.; Kunimoto, K.; Susumu, K.; Taniguchi, M.; Shimidzu, T. *J. Am. Chem. Soc.* **1994**, *116*, 11193.
(10) Susumu, K.; Kunimoto, K.; Segawa, H.; Shimidzu, T. *J. Phys. Chem.* **1995**, *99*, 29.
(11) Shimidzu, T.; Segawa, H.; Wu, F.; Nakayama, N. *J. Photochem. Photobiol. A.: Chem.* **1995**, *92*, 121.
(12) Susumu, K.; Kunimoto, K.; Segawa, H.; Shimidzu, T. *J. Photochem. Photobiol. A.: Chem.* **1995**, *92*, 39.
(13) Susumu, K.; Segawa, H.; Shimidzu, T. *Chem. Lett.* **1995**, 929.
(14) Segawa, H.; Nakayama, N.; Wu, F.; Shimidzu, T. *Synth. Metals* **1993**, *55−57*, 966.
(15) Rao, T. A.; Maiya, B. G. *J. Chem. Soc., Chem. Commun.* **1995**, 939.
(16) Liu, Y. H.; Bénassy, M.-F.; Chojnacki, S.; D'Souza, F.; Barbour, T.; Belcher, W. J.; Brothers, P. J.; Kadish, K. M. *Inorg. Chem.* **1994**, *33*, 4480.
(17) Segawa, H.; Nakayama, N.; Shimidzu, T. *J. Chem. Soc., Chem. Commun.* **1992**, 784.
(18) Kadish, K. M.; Autret, M.; Ou, Z.; Akiba, K.-y.; Masumoto, S.; Wada, R.; Yamamoto, Y. *Inorg. Chem.* **1996**, *35*, 5564.
(19) Fuhrhop, J.-H.; Kadish, K. M.; Davis, D. G. *J. Am. Chem. Soc.* **1973**, *95*, 5140.
(20) Richoux, M. C.; Neta, P.; Harriman, A.; Baral, S.; Hambright, P. *J. Phys. Chem.* **1986**, *90*, 2462.
(21) Shiragami, T.; Kubomura, K.; Ishibashi, D.; Inoue, H. *J. Am. Chem. Soc.* **1996**, *118*, 6311.
(22) Takagi, S.; Okamoto, T.; Shiragami, T.; Inoue, H. *J. Org. Chem.* **1994**, *59*, 7373.
(23) Inoue, H.; Okamoto, T.; Kameo, Y.; Sumitani, M.; Fujiwara, A.; Ishibashi, D.; Hida, M. *J. Chem. Soc., Perkin Trans. 1* **1994**, 105.

10.1021/ic010595e CCC: $20.00
Published on Web 09/25/2001

In a preliminary communication on phosphorus porphyrins, we reported that axial ligands had a profound effect on the degree of ruffling of the porphyrin core,[28] and we now describe full experimental details for preparation of twenty nine phosphorus(V) octaethylporphyrin derivatives of the type $[P(OEP)(X)(Y)]^+Z^-$ (OEP: octaethylporphyrin) (X = CH_3, CH_2CH_3, C_6H_5, F; Y = CH_3, CH_2CH_3, OH, OCH_3, OCH_2CH_3, O*n*-Pr, O*i*-Pr, O*sec*-Bu, NHBu, NEt_2, Cl, F, O^-; Z = ClO_4, PF_6), including X-ray crystallographic analysis of eleven compounds. We were able to prepare a variety of phosphorus(V) octaethylporphyrin derivatives with procedures recently developed by us for the introduction of alkyl substituents at the porphyrin metal by use of trialkylaluminum,[18,29−33] and for introduction of a fluorine atom from counteranions such as PF_6^-,[18,30,33] and thus led to our initial isolation of the quite unique neutral compound, $P(OEP)(CH_2CH_3)(O)$ **3b**.[28] The X-ray analysis of eleven different phosphorus porphyrins clearly reveals that as the axial ligands become more electronegative, the degree of ruffling of the porphyrin core becomes greater and the average P−N bond distance becomes shorter. Therefore, the electronic effects of the axial substituents will play a major role in determining the degree of ruffling, although the steric effects of the substituents also play some role. ^{1}H NMR chemical shifts of a series of $[P(OEP)(CH_2CH_3)(Y)]^+Z^-$ derivatives are strongly affected by the ruffling of the core and the magnitude of the effect can be estimated based on a comparison of the chemical shifts in phosphorus porphyrins with values of the corresponding arsenic porphyrins, where only planar structures have been observed.[31,32]

Because the PO bond length in $P(OEP)(CH_2CH_3)(O)$ **3b** is very short (1.475(7) Å)[28] and the PO bond can be regarded as a double bond, **3b** then becomes the first experimental example of a hypervalent 12-P-6 compound bearing a P═O double bond. During the past few years, there has been widespread interest in hypervalent phosphorus compounds, with a focus on the nature of the bond in phosphine oxides[34−48] and the PO bond has been of general interest.[49,50] To compare the PO bond in regular phosphine oxides such as $(CH_3)_3PO$ with that in $P(OEP)(CH_2CH_3)(O)$ (**3b**), a density functional calculation of $(Por)P(CH_2CH_3)(O)$ (**12b**) (Por: unsubstituted porphyrin) is carried out and the PO bond order and the bond energy are calculated. In addition, a topological analysis of electron density based on *Atoms in Molecules* theory is applied to evaluate the nature of the PO bond. These results indicate that the PO bond in **12b** is very polar and isotropic and is similar to that in $(CH_3)_3PO$. The bond order and the bond energy calculation show that the PO bond in **12b** is slightly weaker than that in $(CH_3)_3PO$. Electrochemistry, spectroelectrochemistry, and ESR spectroscopy of the singly reduced phosphorus(V) octaethylporphyrins are discussed in relation with the corresponding antimony(V) porphyrins[18] and other porphyrin derivatives.[51−58]

Experimental Section

Instrumentation. Cyclic voltammetry was carried out with an EG&G Model 173 potentiostat or an IBM Model EC 225 Voltammetric Analyzer. Current−voltage curves were recorded on an EG&G Princeton Applied Research Model Re-0151 X-Y recorder. A three-electrode system was used and consisted of a glassy carbon or platinum button working electrode, a platinum wire counter electrode, and a saturated calomel reference electrode (SCE). This reference electrode was separated from the bulk of the solution by a fritted-glass bridge filled with the solvent/supporting electrolyte mixture. All potentials are referenced to the SCE. UV−vis spectroelectrochemical experiments were performed with a home-built platinum thin-layer electrode of the type described in the literature.[59] Potentials were applied and monitored with an EG&G Princeton Applied Research Model 173 potentiostat. Time-resolved UV−vis spectra were recorded with a HP 8453 UV−vis spectrophotometer.

Melting points were measured with a Yanagimoto micromelting point apparatus and were uncorrected. ^{1}H NMR (400 MHz), ^{19}F NMR (376 MHz), and ^{13}C NMR (100 MHz) spectra were recorded on a JEOL EX-400 spectrometer. ^{1}H NMR (90 MHz) and ^{19}F NMR (85 MHz) spectra were recorded on a Hitachi R-90H spectrometer. Chemical shifts are reported (δ scale) with respect to internal tetramethylsilane for the ^{1}H and ^{13}C spectra or with respect to fluorotrichloromethane for the ^{19}F spectra. UV−vis spectra were recorded on a Shimadzu UV-2200 spectrophotometer. Elemental analyses were performed on a Perkin-Elmer 2400 CHN elemental analyzer. Column chromatography was carried out using Merck neutral alumina 1077.

Chemicals. Benzonitrile (PhCN) was purchased from Aldrich Chemical Co. and distilled over P_2O_5 under vacuum prior to use. Absolute dichloromethane (CH_2Cl_2) was obtained over molecular sieves from Fluka Chemical Co. and was used without further purification. Tetra-*n*-butylammonium perchlorate (TBAP) was purchased from

(24) Okamoto, T.; Takagi, S.; Shiragami, T.; Inoue, H. *Chem. Lett.* **1993**, 687.
(25) Takagi, S.; Okamoto, T.; Shiragami, T.; Inoue, H. *Chem. Lett.* **1993**, 793.
(26) Inoue, H.; Okamoto, T.; Komiyama, M.; Hida, M. *J. Photochem. Photobiol. A.: Chem.*, **1992**, *65*, 221.
(27) Inoue, H.; Sumitani, M.; Sekita, A.; Hida, M. *J. Chem. Soc., Chem. Commun.* **1987**, 1681.
(28) Yamamoto, Y.; Nadano, R.; Itagaki, M. and Akiba, K.-y. *J. Am. Chem. Soc.* **1995**, *117*, 8287.
(29) Akiba, K.-y.; Onzuka, Y.; Itagaki, M.; Hirota, H.; Yamamoto, Y. *Organometallics*, **1994**, *13*, 2800.
(30) Satoh, W.; Masumoto, S.; Shimizu, M.; Yamamoto, Y.; Akiba, K.-y. *Bull. Chem. Soc. Jpn.*, **1999**, *73*, 459.
(31) Satoh, W.; Nadano, R.; Yamamoto, Y.; Akiba, K.-y. *Chem. Commun.*, **1996**, 2451.
(32) Satoh, W.; Nadano, R.; Yamamoto, G.; Yamamoto, Y.; Akiba, K.-y. *Organometallics*, **1997**, *16*, 3664.
(33) Yamamoto, A.; Satoh, W.; Yamamoto, Y.; Akiba, K.-y. *Chem. Commun.*, **1999**, 147.
(34) Dobado, J. A.; Martínez-García, H.; Molina, J. M.; Sundberg, M. R. *J. Am. Chem. Soc.* **1998**, *120*, 8461.
(35) Keil, F.; Kutzelnigg, W. *J. Am. Chem. Soc.* **1975**, *97*, 3623.
(36) Kutzelnigg, W. *Pure Appl. Chem.* **1977**, *49*, 981.
(37) Wallmeier, H.; Kutzelnigg, W. *J. Am. Chem. Soc.* **1979**, *101*, 2804.
(38) Kutzelnigg, W. *Angew. Chem., Int. Ed. Engl.* **1984**, *23*, 272.
(39) Gordon, M. S.; Boatz, J. A.; Schmidt, M. W. *J. Phys. Chem.* **1984**, *88*, 2998.
(40) Schmidt, M. W.; Gordon, M. S. *J. Am. Chem. Soc.* **1985**, *107*, 1922.
(41) Bollinger, J. C.; Houriet, R.; Kern, C. W.; Perret, D.; Weber, J.; Yvernault, T. *J. Am. Chem. Soc.* **1985**, *107*, 5352.
(42) Boatz, J. A.; Gordon, M. S. *J. Comput. Chem.* **1986**, *7*, 306.
(43) Streitwieser, A.; McDowell, R. S.; Glaser, R. *J. Comput. Chem.* **1987**, *8*, 788.
(44) Streitwieser, A.; Rajca, A.; McDowell, R. S.; Glaser, R. *J. Am. Chem. Soc.* **1987**, *109*, 4184.
(45) Liang, C.; Allen, L. C. *J. Am. Chem. Soc.* **1987**, *109*, 6449.
(46) Schneider, W.; Thiel, W.; Komornicki, A. *J. Phys. Chem.* **1988**, *92*, 5611.
(47) Reed, A. E.; Schleyer, P. v. R. *J. Am. Chem. Soc.* **1990**, *112*, 1434.
(48) Messmer, R. P. *J. Am. Chem. Soc.* **1991**, *113*, 433.
(49) Gilheany, D. G. *The Chemistry of Organophosphorous Compounds*; Wiley-Interscience: Chichester, 1992; Vol. 2.
(50) Gilheany, D. G. *Chem. Rev.* **1994**, *94*, 1339.
(51) Kadish, K. M.; Boisselier-Cocolios, B.; Cocolios, P.; Guilard, R. *Inorg. Chem.* **1985**, *24*, 2139.
(52) Kadish, K. M.; Boisselier-Cocolios, B.; Coutsolelos, A.; Mitaine, P.; Guilard, R. *Inorg. Chem.* **1985**, *24*, 4521.
(53) Tabard, A.; Guilard, R.; Kadish, K. M.*Inorg. Chem.* **1986**, *25*, 4277.
(54) Kadish, K. M.; Tabard, A.; Zrineh, A.; Ferhat, M.; Guilard, R. *Inorg. Chem.* **1987**, 26, 2459.
(55) Kadish, K. M.; Xu, Q. Y.; Barbe, J.-M.; Anderson, J. E.; Wang, E.; Guilard, R. *J. Am. Chem. Soc.* **1987**, *109*, 7705.
(56) Guilard, R.; Lecomte, C.; Kadish, K. M. *Struct. Bonding (Berlin)* **1987**, *64*, 205.
(57) Guilard, R.; Kadish, K. M. *Chem. Rev.* **1988**, *88*, 1121.
(58) Kadish, K. M.; Xu, Q. Y.; Barbe, J.-M.; Guilard, R. *Inorg. Chem.* **1988**, *27*, 1191.
(59) Lin, X. Q.; Kadish, K. M. *Anal. Chem.* **1985**, *57*, 1498.

Sigma Chemical Co., recrystallized from ethanol and dried under vacuum at 40 °C for at least one week prior to use.

[P(OEP)(Cl)$_2$]$^+$PF$_6^-$ (1-PF$_6$) and General Procedure for Counteranion Exchange. A solution of (OEP)H$_2$ (1.86 g, 3.48 mmol) and PCl$_3$ (4.60 mL, 52.7 mmol) in dry dichloromethane (80 mL) and 2,6-dimethylpyridine (20 mL) was stirred for 1 day at room temperature under Ar. Water (20 mL) and dichloromethane (50 mL) were added to the solution. Extraction, removal of the solvent in vacuo, and purification by chromatography (acetonitrile) gave [P(OEP)(Cl)$_2$]$^+$Cl$^-$ (**1**-Cl). Conteranion exchange was carried out by dissolving **1**-Cl in dichloromethane and potassium hexafluorophosphate (5 equiv) in dichloromethane was added to the solution. After the mixture was stirred for 10 h, pure [P(OEP)(Cl)$_2$]$^+$PF$_6^-$ (**1**-PF$_6$, 490 mg, 45%) was obtained by extraction with dichloromethane/water followed by recrystallization from dichloromethane/*n*-hexane (1:1). **1**-PF$_6$: ^{1}H NMR (CDCl$_3$) δ 1.87 (t, 24 H, J = 7.8 Hz), 3.95 (q, 16 H, J = 7.8 Hz), 9.66 (d, 4 H, J = 1.5 Hz). ^{31}P NMR (CDCl$_3$) δ −228.6 (s), −144.6 (sept, J = 714 Hz). Anal. Calcd for C$_{36}$H$_{44}$N$_4$Cl$_2$P$_2$F$_6$: C, 55.46; H, 5.69; N, 7.19. Found: C, 55.86; H, 5.93; N, 6.82.

Preparation of [P(OEP)(R)(OH)]$^+$Z$^-$. A solution of (OEP)H$_2$ (480 mg, 0.897 mmol) and RPCl$_2$ (2.2 mmol) in dry dichloromethane (20 mL) and 2,6-dimethylpyridine (0.5 mL) was heated under reflux for 1.5 days under Ar. After evaporation of the solvent, the residue was dissolved in CH$_3$CN (5 mL) and CH$_2$Cl$_2$ (20 mL). H$_2$O (5 mL) and Al$_2$O$_3$ (1 g) were added to the mixture which was then stirred for 12 h at room temperature and filtered through Celite. Extraction, removal of the solvent in vacuo, and purification by chromatography (benzene/methyl acetate/methanol; 15:15:1) gave a purple solid. The solid was dissolved in CH$_2$Cl$_2$ (40 mL) and the solution washed with aqueous HCl (30 mL, pH 3) to give [P(OEP)(CH$_3$)(OH)]$^+$Cl$^-$. A small amount of (OEP)H$_2$ was removed by crystallization (methanol/CH$_2$Cl$_2$). Pure [P(OEP)(CH$_3$)(OH)]$^+$Cl$^-$ (210 mg, 37%) was obtained by recrystallization (CH$_2$Cl$_2$/*n*-hexane; 1:1). Conteranion exchange was carried out (see general procedure).

[P(OEP)(CH$_3$)(OH)]$^+$PF$_6^-$ (2a-PF$_6$). 37% Yield; mp 267−269 °C (CH$_2$Cl$_2$/*n*-hexane; 1:1). UV−vis (CH$_2$Cl$_2$) λ ($\epsilon \times 10^{-3}$) 358 (27.2), 417 (277), 548 (13.0), 589 nm (14.7); ^{1}H NMR (CDCl$_3$) δ −5.74 (d, 3 H, J = 14.7 Hz), 1.91 (t, 24 H, J = 7.5 Hz), 4.02 (q, 16 H, J = 7.5 Hz), 9.68 (s, 4 H); ^{31}P NMR (CDCl$_3$) δ -194.4 (s), −144.4 (sept, J = 714 Hz). Anal. Calcd for C$_{37}$H$_{48}$N$_4$OP$_2$F$_6$·CH$_2$Cl$_2$: C, 55.28; H, 6.10; N, 6.79. Found: C, 55.31; H, 6.08; N, 6.63.

[P(OEP)(CH$_2$CH$_3$)(OH)]$^+$ClO$_4^-$ (2b-ClO$_4$). 50% Yield; mp 219−235 °C (CH$_2$Cl$_2$/ethyl acetate; 1:1). UV−vis (CH$_2$Cl$_2$) λ ($\epsilon \times 10^{-3}$) 357 (26.9), 418 (274), 548 (13.3), 590 (14.1). ^{1}H NMR (CDCl$_3$) δ −5.70 (dq, 2 H, J = 12.0, 7.5 Hz), −4.52 (dt, 3 H, J = 41.8, 7.5 Hz), 1.91 (t, 24 H, J = 7.5 Hz), 4.03 (q, 16 H, J = 7.5 Hz), 9.72 (s, 4 H). ^{31}P NMR (CDCl$_3$) δ −179.8 (s). ^{13}C NMR (CDCl$_3$) δ 5.54 (d, J = 9.0 Hz), 17.91 (d, J = 19.6 Hz), 39.80 (d, J = 202 Hz), 94.23 (s), 138.1 (s), 144.0 (s). Anal. Calcd for C$_{38}$H$_{50}$N$_4$O$_5$Cl·0.5AcOEt: C, 63.77; H, 7.23; N, 7.44. Found: C, 63.57; H, 7.27; N,7.39.

[P(OEP)(C$_6$H$_5$)(OH)]$^+$PF$_6^-$ (2c-PF$_6$). 93% Yield; mp 227−231 °C (CH$_2$Cl$_2$/*n*-hexane; 1:1). UV−vis (CH$_2$Cl$_2$) λ ($\epsilon \times 10^{-3}$) 357 (20.8), 417 (246), 550 (11.3), 592 (15.0). ^{1}H NMR (CDCl$_3$) δ −3.79 (s, 1 H), 0.53 (dd, 2 H, J = 24.2, 7.9 Hz), 1.81 (t, 24 H, J = 7.6 Hz), 3.92 (dq, 8 H, J = 15, 7.6 Hz), 3.9−4.1 (bm, 8 H), 4.78 (ddd, 2 H, J = 7.9, 7.9, 7.9 Hz), 5.47 (dt, 1 H, J = 4.4, 7.9 Hz), 9.43 (bs, 4 H). ^{31}P NMR (CDCl$_3$) δ −194.1 (s), −144.3 (sept, J = 714 Hz). Anal. Calcd for C$_{42}$H$_{50}$N$_4$OP$_2$F$_6$·0.5CH$_2$Cl$_2$: C, 60.39; H, 6.08; N, 6.63. Found: C, 60.37; H, 6.32; N, 6.49.

Preparation of P(OEP)(R)(O). A solution of [P(OEP)(R)(OH)]$^+$Cl$^-$ (17.0 μmol) in dichloromethane (30 mL) was washed with aqueous Na$_2$CO$_3$ (70 mL, pH 11) and the solvent then evaporated. P(OEP)(R)(O) was obtained quantitatively.

P(OEP)(CH$_3$)(O) (3a). UV−vis (CH$_2$Cl$_2$) λ ($\epsilon \times 10^{-3}$) 346 (31.0), 416 (189), 539 (15.4), 573 (12.2). ^{1}H NMR (CDCl$_3$) δ −6.37 (bd, 3 H), 1.90 (bt, 24 H), 4.02 (bdq, 8 H), 4.08 (bdq, 8 H), 9.95 (bs, 4 H). ^{31}P NMR (CDCl$_3$) δ −150.3 (s).

P(OEP)(CH$_2$CH$_3$)(O) (3b). UV−vis (CH$_2$Cl$_2$) λ ($\epsilon \times 10^{-3}$) 347 (27.6), 417 (166.5), 539 (12.9), 572 (9.68). ^{1}H NMR (CDCl$_3$) δ −6.39 (bdq, 2 H), −5.08 (bdt, 3 H), 1.80 (bt, 24 H), 4.02 (bdq, 8 H), 4.06 (bdq, 8 H), 10.20 (bs, 4 H). ^{31}P NMR (CDCl$_3$) δ −131.4 (s). ^{13}C NMR (CDCl$_3$) δ 5.79 (d, J = 11.0 Hz), 18.37 (d, J = 19.8 Hz), 49.26 (d, J = 254 Hz), 95.16 (s), 139.7 (s), 140.6 (s).

P(OEP)(C$_6$H$_5$)(O) (3c). UV−vis (CH$_2$Cl$_2$) λ ($\epsilon \times 10^{-3}$) 350 (27.7), 419 (160), 542 (13.1), 580 (12.7). ^{1}H NMR (CDCl$_3$) δ −0.02 (bdd, 2 H), 1.84 (bt, 24 H), 3.90 (bdq, 8 H), 4.00 (bdq, 8 H), 4.54 (bdt, 2 H), 5.18 (bdt, 1 H), 9.60 (bs, 4 H). ^{31}P NMR (CDCl$_3$) δ −163.1 (s).

Preparation of [P(OEP)(R)(OR′)]$^+$Z$^-$. PCl$_3$ (0.1 mL, 1.1 mmol) was added to a solution of [P(OEP)(R)(OH)]$^+$Cl$^-$ (10 μmol) in 0.6 mL of dry dichloromethane under Ar. The mixture was stirred for 7 days and the solvent then evaporated to give crude [P(OEP)(R)(Cl)]$^+$Cl$^-$. R′OH (2.5 mmol) and dichloromethane (0.5 mL) were added and the solution was stirred for 2 h at room temperature. The solvent was evaporated and the residue chromatographed (benzene/methyl acetate/methanol; 15:15:1) to give [P(OEP)(R)(OR′)]$^+$Cl$^-$. Counteranion exchange was carried out (see general procedure).

[P(OEP)(CH$_3$)(OCH$_3$)]$^+$PF$_6^-$ (6a-PF$_6$). 37% Yield; mp 200−220 °C (CH$_2$Cl$_2$/*n*-hexane; 1:1): ^{1}H NMR (CDCl$_3$) δ −5.69 (d, 3 H, J = 14.7 Hz), −2.91 (d, 3 H, J = 29.4 Hz), 1.92 (t, 24 H, J = 7.5 Hz), 4.08 (q, 16 H, J = 7.5 Hz), 9.76 (s, 4 H). ^{31}P NMR (CDCl$_3$) δ −185.6 (s). Anal. Calcd for C$_{38}$H$_{50}$N$_4$OP$_2$F$_6$: C, 60.47; H, 6.68; N, 7.42. Found: C, 60.57; H, 6.66; N, 7.48.

[P(OEP)(CH$_2$CH$_3$)(O*i*-Pr)]$^+$ClO$_4^-$ (6b-ClO$_4$). 50% Yield; mp 214−230 °C (CH$_2$Cl$_2$/ethyl acetate; 1:1). UV−vis (CH$_2$Cl$_2$) λ ($\epsilon \times 10^{-3}$) 357 (30.0), 419 (237), 546 (13.2), 587 nm (13.5). ^{1}H NMR (CDCl$_3$) δ −6.07 (dq, 2 H, J = 11.0, 7.3 Hz), −4.81 (dt, 3 H, J = 42.6, 7.3 Hz), −3.85 (dsept, 1 H, J = 28.6, 6.0 Hz), −2.88 (d, 6 H, J = 6.0 Hz), 1.81 (t, 24 H, J = 7.3 Hz), 4.05 (q, 16 H, J = 7.3 Hz), 9.88 (s, 4 H). ^{31}P NMR (CDCl$_3$) δ −169.1 (s). Anal. Calcd for C$_{41}$H$_{56}$N$_4$O$_5$PCl: C, 65.54; H, 7.51; N, 7.46. Found: C, 65.23; H, 7.60; N, 7.52.

[P(OEP)(CH$_2$CH$_3$)(O*sec*-Bu)]$^+$ClO$_4^-$ (6c-ClO$_4$). 58% Yield; mp 210−230 °C (CH$_2$Cl$_2$/*n*-hexane; 1:1): UV−vis (CH$_2$Cl$_2$) λ ($\epsilon \times 10^{-3}$) 358 (30.5), 419 (242), 546 (13.5), 586 nm (13.7). ^{1}H NMR (CDCl$_3$) δ −6.01 (dq, 2 H, J = 11.0, 7.3 Hz), −4.74 (dt, 3 H, J = 42.6, 7.3 Hz), −3.99 (dddq, 1 H, J = 28.6, 7.3, 7.3, 7.3 Hz), −2.99 (m, 1 H), −2.94 (d, 3 H, J = 7.3 Hz), −2.63 (ddq, 1 H, J = 14.6, 7.3, 7.3 Hz), −1.61 (dd, 3 H, J = 7.3, 7.3 Hz), 1.89 (t, 24 H, J = 7.2 Hz), 4.12 (dq, 8 H, J = 14.5, 7.2 Hz), 4.14 (dq, 8 H, J = 14.5, 7.2 Hz), 9.98 (s, 4 H). ^{31}P NMR (CDCl$_3$) δ −168.2 (s). Anal. Calcd for C$_{42}$H$_{58}$N$_4$O$_5$PCl: C, 65.91; H, 7.64; N, 7.32. Found: C, 66.05; H, 7.59; N, 7.36.

[P(OEP)(C$_6$H$_5$)(OCH$_3$)]$^+$ClO$_4^-$ (6d-ClO$_4$). 67% Yield; mp 270−300 °C (CH$_2$Cl$_2$/*n*-hexane; 1:1). UV−vis (CH$_2$Cl$_2$) λ ($\epsilon \times 10^{-3}$) 357 (23.7), 419 (247), 551 (11.6), 595 nm (16.6). ^{1}H NMR (CDCl$_3$) δ −2.52 (d, 3 H, J = 27.9 Hz), 0.59 (dd, 2 H, J = 23.5, 8.1 Hz), 1.80 (t, 24 H, J = 7.4 Hz), 3.97 (dq, 8 H, J = 14.9, 7.4 Hz), 4.0−4.1 (bm, 8 H), 4.80 (ddd, 2 H, J = 7.7, 7.7, 7.7 Hz), 5.49 (dt, 1 H, J = 4.4, 7.7 Hz), 9.49 (s, 4 H). ^{31}P NMR (CDCl$_3$) δ −185.7 (s).

[P(OEP)(C$_6$H$_5$)(OCH$_2$CH$_3$)]$^+$ClO$_4^-$ (6e-ClO$_4$). 69% Yield; mp 248−255 °C (CH$_2$Cl$_2$/*n*-hexane; 1:1). UV−vis (CH$_2$Cl$_2$) λ ($\epsilon \times 10^{-3}$) 358 (24.7), 419 (253), 551 (11.8), 594 nm (16.4). ^{1}H NMR (CDCl$_3$) δ −2.93 (dq, 2 H, J = 16.5, 7.0 Hz), −2.19 (dt, 3 H, J = 2.2, 7.0 Hz), 0.56 (dd, 2 H, J = 23.5, 7.8 Hz), 1.78 (t, 24 H, J = 7.2 Hz), 3.98 (dq, 8 H, J = 14.4, 7.2 Hz), 4.0−4.1 (bm, 8 H), 4.78 (ddd, 2 H, J = 7.8, 7.8, 7.8 Hz), 5.47 (dt, 1 H, J = 3.6, 7.8 Hz), 9.48 (bs, 4 H). ^{31}P NMR (CDCl$_3$) δ −186.8 (s). Anal. Calcd for C$_{44}$H$_{54}$N$_4$O$_5$PCl: C, 67.29; H, 6.93; N, 7.14. Found: C, 67.16; H, 6.97; N, 7.09.

[P(OEP)(C$_6$H$_5$)(OCH$_2$CH$_2$CH$_3$)]$^+$ClO$_4^-$ (6f-ClO$_4$). 49% Yield; mp >300 °C (CH$_2$Cl$_2$/ethyl acetate/*n*-heptane; 1:1:1). UV−vis (CH$_2$Cl$_2$) λ ($\epsilon \times 10^{-3}$) 358 (24.7), 420 (254), 552 (12.0), 594 nm (16.6). ^{1}H NMR (CDCl$_3$) δ −3.09 (dt, 2 H, J = 13.2, 6.9 Hz), −1.89 (tq, 2 H, J = 6.9, 6.9 Hz), −1.45 (t, 2 H, J = 6.9 Hz), 0.53 (dd, 2 H, J = 23.5, 7.7 Hz), 1.78 (t, 24 H, J = 7.5 Hz), 3.98 (dq, 8 H, J = 15.1, 7.5 Hz), 4.0−4.1 (bm, 8 H), 4.77 (ddd, 2 H, J = 7.7, 7.7, 7.7 Hz), 5.46 (dt, 1 H, J = 3.7, 7.7 Hz), 9.49 (s, 4 H). ^{31}P NMR (CDCl$_3$) δ −186.7 (s). Anal. Calcd for C$_{45}$H$_{56}$N$_4$O$_5$PCl: C, 67.61; H, 7.06; N, 7.01. Found: C, 67.36; H, 7.17; N, 7.00.

[P(OEP)(C$_6$H$_5$)(O*i*-Pr)]$^+$ClO$_4^-$ (6g-ClO$_4$). 43% Yield; mp 241−245 °C (CH$_2$Cl$_2$/*n*-heptane; 1:1). UV−vis (CH$_2$Cl$_2$) λ ($\epsilon \times 10^{-3}$) 356 (26.0), 419 (255), 548 (12.2), 590 nm (16.4). ^{1}H NMR (CDCl$_3$) δ −3.15 (dsept, 1 H, J = 38.6, 6.0 Hz), −2.47 (d, 6 H, J = 6.0 Hz), 0.21 (dd, 2 H, J = 23.8, 8.1 Hz), 1.79 (t, 24 H, J = 7.3 Hz), 4.01 (dq, 8 H, J = 14.7, 7.3 Hz), 4.07 (dq, 8 H, J = 14.7, 7.3 Hz), 4.69 (ddd, 2 H, J =

8.1, 8.1, 8.1 Hz), 5.39 (dt, 1 H, J = 4.4, 8.1 Hz), 9.65 (s, 4 H). ^{31}P NMR ($CDCl_3$) δ −184.8 (s). Anal. Calcd for $C_{45}H_{56}N_4O_5PCl$: C, 67.61; H, 7.06; N, 7.01. Found: C, 67.28; H, 6.82; N, 6.97.

[P(OEP)(C_6H_5)(Cl)]$^+$Cl$^-$ (4c-Cl). PCl_5 (37.1 mg, 178 μmol) was added to 0.6 mL of [P(OEP)(C_6H_5)(OH)]$^+$Cl$^-$ (6.9 mg, 11 mmol) in dry dichloromethane and the solution stirred for 22 h at room temperature. The solvent was evaporated in vacuo and $CDCl_3$ (0.5 mL) was added to the residue. **4c-Cl**: UV−vis (CH_2Cl_2) λ ($\epsilon \times 10^{-3}$) 362, 424, 557, 600 nm. ^{1}H NMR ($CDCl_3$) δ 0.86 (bs, 2 H), 1.82 (bs, 24 H), 3.97 (bs, 16 H), 4.98 (bs, 2 H), 5.62 (bs, 1 H), 8.9−10.0 (bd, 4 H). ^{31}P NMR ($CDCl_3$) δ −212.9 (s).

Preparation of [P(OEP)(CH_2CH_3)(N(R′)(R"))]$^+$$ClO_4^-$. PCl_3 (1.0 mL, 12 mmol) was added to a solution of [P(OEP)(CH_2CH_3)(OH)]$^+$Cl$^-$ (86.3 mg, 134 μmol) in dry dichloromethane (5 mL), the solution was stirred for 12 h at 30 °C and the solvent then evaporated. Amine (4.8 mmol) and dichloromethane (5 mL) were added and the reaction mixture was stirred for 20 min at room temperature. After the solvent was evaporated, the residue was chromatographed (benzene/methyl acetate/methanol; 15:15:1) to give [P(OEP)(CH_2CH_3)(N(CH_2CH_3)$_2$)]$^+$Cl$^-$. Counteranion exchange with sodium perchlorate was carried out.

[P(OEP)(CH_2CH_3)(N(CH_2CH_3)$_2$)]$^+$$ClO_4^-$ (7a-ClO_4). 12% Yield; mp 218−222 °C (CH_2Cl_2/ethyl acetate; 1:1). UV−vis (CH_2Cl_2) λ ($\epsilon \times 10^{-3}$) 364 (36.5), 421 (213), 550 (13.0), 589 nm (11.1). ^{1}H NMR ($CDCl_3$) δ −5.92 (dq, 2 H, J = 12.3, 6.9 Hz), −4.67 (dt, 3 H, J = 42.6, 6.9 Hz), −4.04 (dq, 4 H, J = 20.5, 6.8 Hz), −2.59 (t, 6 H, J = 6.8 Hz), 1.87 (t, 24 H, J = 7.5 Hz), 4.09 (bq, 16 H, J = 7.5 Hz), 9.81 (s, 4 H). ^{31}P NMR ($CDCl_3$) δ −170.4 (s). ^{13}C NMR ($CDCl_3$) δ 6.06 (d, J = 11.0 Hz), 18.11 (d, J = 19.6 Hz), 43.20 (d, J = 232 Hz), 94.56 (s), 138.8 (s), 144.1 (s). Anal. Calcd for $C_{42}H_{59}N_5O_4PCl$: C, 65.99; H, 7.78; N, 9.17. Found: C, 66.42; H, 7.84; N, 9.17.

[P(OEP)(CH_2CH_3)(NH($CH_2CH_2CH_2CH_3$))]$^+$$ClO_4^-$ (7b-ClO_4). 12% Yield; mp 200−220 °C (CH_2Cl_2/*n*-hexane; 1:1): ^{1}H NMR ($CDCl_3$) δ −6.45 (s, 1 H), −5.88 (dq, 2 H, J = 11.5, 7.3 Hz), −4.66 (dt, 3 H, J = 44.0, 7.3 Hz), −4.13 (dt, 2 H, J = 11.7, 7.0 Hz), −2.14 (tt, 2 H, J = 7.0, 7.0 Hz), −1.32 (tq, 2 H, J = 7.0, 7.0 Hz), −0.54 (t, 3 H, J = 7.0 Hz), 1.91 (t, 24 H, J = 7.5 Hz), 4.11 (q, 16 H, J = 7.5 Hz), 9.87 (s, 4 H). ^{31}P NMR ($CDCl_3$) δ −174.0 (s). Anal. Calcd for $C_{42}H_{59}N_5O_4PCl$: C, 65.99; H, 7.78; N, 9.17. Found: C, 65.91; H, 7.73; N, 9.00.

Preparation of [P(OEP)(R)(F)]$^+$$PF_6^-$. $(COBr)_2$ (0.3 mL, 2.1 mmol) was added to a solution of [P(OEP)(R)(OH)]$^+$$PF_6^-$ (59 mg, 98 μmol) in 10 mL of dichloromethane and the reaction mixture was stirred for 3 h at room temperature. The solvent was evaporated and the residue was chromatographed (benzene/methyl acetate/methanol; 15:15:1). Counteranion exchange with potassium hexafluorophosphate was carried out.

[P(OEP)(CH_3)(F)]$^+$$PF_6^-$ (9a-PF_6). 42% Yield; mp 243−248 °C (CH_2Cl_2/ethyl acetate/*n*-heptane; 1:1:1). UV−vis (CH_2Cl_2) λ ($\epsilon \times 10^{-3}$) 357 (19.3), 417 (268), 547 (11.5), 590 (16.4). ^{1}H NMR ($CDCl_3$) δ −5.58 (d, 3 H, J = 13.5 Hz), 1.87 (t, 24 H, J = 7.5 Hz), 3.99 (q, 16 H, J = 7.5 Hz), 9.59 (s, 4 H). ^{31}P NMR ($CDCl_3$) δ −193.7 (d, J = 798 Hz), −144.3 (sept, J = 712 Hz). ^{19}F NMR ($CDCl_3$) δ -74.3 (d, 6 F, J = 712 Hz), −18.4 (d, 1 F, J = 798 Hz). Anal. Calcd for $C_{37}H_{47}N_4P_2F_7 \cdot 0.5CH_2Cl_2$: C, 57.36; H, 6.16; N, 7.13. Found: C, 57.48; H, 6.42; N, 6.98.

[P(OEP)(CH_2CH_3)(F)]$^+$$PF_6^-$ (9b-PF_6). 21% Yield; mp 253−256 °C (CH_2Cl_2/*n*-hexane; 1:1). UV−vis (CH_2Cl_2) λ ($\epsilon \times 10^{-3}$) 358 (23.2), 415 (283), 549 (12.1), 592 (16.4). ^{1}H NMR ($CDCl_3$) δ −5.32 (dq, 2 H, J = 15, 7.5 Hz), −4.25 (dt, 3 H, J = 39.6, 7.5 Hz), 1.88 (t, 24 H, J = 7.7 Hz), 3.9−4.1 (m, 16 H), 9.64 (s, 4 H). ^{31}P NMR ($CDCl_3$) δ −180.4 (d, J = 766 Hz), −144.2 (sept, J = 713 Hz). ^{19}F NMR ($CDCl_3$) δ -74.6 (d, 6 F, J = 713 Hz), −19.2 (d, 1 F, J = 766 Hz). Anal. Calcd for $C_{38}H_{49}N_4P_2F_7 \cdot 0.5$hexane: C, 60.96; H, 6.80; N, 7.20. Found: C, 61.34; H, 6.59; N, 7.34.

[P(OEP)(C_6H_5)(F)]$^+$$PF_6^-$ (9c-PF_6). In this case CH_3CN (5 mL) and *tert*-butyl alcohol (1 mL) were used as solvents. 64% yield; mp >300 °C (CH_2Cl_2/*n*-heptane; 1:1). UV−vis (CH_2Cl_2) λ ($\epsilon \times 10^{-3}$) 355 (17.6), 413 (259), 548 (11.2), 593 (18.5). ^{1}H NMR ($CDCl_3$) δ 0.87 (dd, 2 H, J = 22.7, 7.8 Hz), 1.78 (bm, 24 H), 3.7−3.9 (bm, 4 H), 3.9−4.0 (bm, 8 H), 4.0−4.4 (bm, 4 H), 4.93 (ddd, 2 H, J = 7.8, 7.8, 7.8 Hz), 5.62 (dt, 1H, J = 3.7, 7.8 Hz), 9.0−9.2 (bs, 2 H), 9.6−9.8 (s, 2 H). ^{31}P NMR ($CDCl_3$) δ −192.3 (d, J = 767 Hz), −143.6 (sept, J = 712 Hz). ^{19}F NMR ($CDCl_3$) δ -74.2 (d, 6 F, J = 712 Hz), −18.8 (d, 1 F, J = 767 Hz). Anal. Calcd for $C_{42}H_{49}N_4P_2F_7$: C, 62.68; H, 6.14; N, 6.96. Found: C, 62.53; H, 6.12; N, 6.57.

[P(OEP)(F)(OH)]$^+$$ClO_4^-$ (2d-ClO_4). Aqueous sodium carbonate (10 mL, pH10) was added to a solution of [P(OEP)($Cl)_2$]$^+$Cl$^-$ (106 mg, 159 μmol) in dichloromethane (10 mL) and the mixture was stirred for 12 h at room temperature. The organic layer was separated and the aqueous layer extracted with dichloromethane (3 × 40 mL). The combined organic layer was washed with aqueous HCl (30 mL, pH 3) and the solvent was evaporated to give crude [P(OEP)($OH)_2$]$^+$Cl$^-$. Counteranion exchange with potassium hexafluorophosphate gave crude [P(OEP)($OH)_2$]$^+$$PF_6^-$. $(COBr)_2$ (0.5 mL, 3.5 mmol) was added to a solution of the crude [P(OEP)($OH)_2$]$^+$$PF_6^-$ in 6 mL of dichloromethane and the reaction mixture was stirred for 2.5 h at room temperature. After the solvent was evaporated the residue was chromatographed (benzene/methyl acetate/methanol; 15:15:1) to give [P(OEP)(F)(O)]. The 40 mL solution of [P(OEP)(F)(O)] in dichloromethane was washed with aqueous HCl (40 mL, pH 3) to give [P(OEP)(F)(OH)]$^+$Cl$^-$. Counteranion exchange with sodium perchlorate gave 59.0 mg (53%) of [P(OEP)(F)(OH)]$^+$ ClO_4^-. Mp 175−182 °C (CH_2Cl_2/*n*-hexane; 1:1). UV−vis (CH_2Cl_2) λ ($\epsilon \times 10^{-3}$) 403 (268), 543 (12.3), 587 nm (21.3). ^{1}H NMR ($CDCl_3$) δ 1.84 (t, 24 H, J = 7.7 Hz), 3.8−4.0 (bm, 16 H), 9.98 (s, 4 H). ^{31}P NMR ($CDCl_3$) δ −191.3 (d, J = 816 Hz). ^{19}F NMR ($CDCl_3$) δ -33.8 (d, 1 F, J = 816 Hz). Anal. Calcd for $C_{36}H_{45}N_4O_5FClP$: C, 61.84; H, 6.49; N, 8.02. Found: C, 62.12; H, 6.69; N, 8.18.

Preparation of P(OEP)(F)(O) (3d). 1,8-Diazabicyclo[5.4.0]undec-7-ene (DBU: 0.04 mL, 0.3 mmol) was added to a solution of [P(OEP)(F)(OH)]$^+$Cl$^-$ (6.9 mg, 11 μmol) in $CDCl_3$ (0.6 mL) at room temperature to give P(OEP)(F)(O). UV−vis (CH_2Cl_2) λ ($\epsilon \times 10^{-3}$) 340 (13.4), 402 (234), 536 (11.6), 576 nm (20.8). ^{1}H NMR ($CDCl_3$) δ 1.81 (t, 24 H, J = 24 Hz), 3.85 (q, 16 H, J = 7.5 Hz), 9.35 (s, 4 H). ^{31}P NMR ($CDCl_3$) δ −173.3 (d, J = 743 Hz). ^{19}F NMR ($CDCl_3$) δ −22.1 (d, 1 F, J = 743 Hz).

[P(OEP)(F)(Cl)]$^+$$PF_6^-$ (4d-PF_6). PCl_5 (0.6 mL, 2.9 mmol) was added to a solution of [P(OEP)(F)(OH)]$^+$$ClO_4^-$ (43.4 mg, 62.1 μmol) in dry dichloromethane (8 mL) under Ar. The mixture was heated under reflux for 1 day and treated with water (20 mL). Extraction, removal of the solvent in vacuo, and purification by chromatography (dichloromethane) gave [P(OEP)(F)(Cl)]$^+$Cl$^-$. Counteranion exchange with potassium hexafluorophosphate gave 20.5 mg (43%) of [P(OEP)-(F)(Cl)]$^+$$PF_6^-$. Mp 269−271 °C ($CH_2Cl_2$/ethyl acetate/*n*-heptane; 1:1:1). UV−vis (CH_2Cl_2) λ ($\epsilon \times 10^{-3}$) 409 (234), 548 (12.3), 592 nm (20.0). ^{1}H NMR ($CDCl_3$) δ 1.84 (bt, 12 H), 1.85 (bt, 12 H), 3.8−4.2 (bm, 16 H), 9.45 (s, 2 H), 9.62 (s, 2 H). ^{31}P NMR ($CDCl_3$) δ −207.8 (d, J = 812 Hz), −143 (sept, J = 712 Hz). ^{19}F NMR ($CDCl_3$) δ -74.0 (d, 6 F, J = 712 Hz), −38.6 (d, 1 F, J = 812 Hz). Anal. Calcd for $C_{36}H_{44}N_4P_2F_7Cl \cdot 0.5CH_2Cl_2$: C, 54.41; H, 5.63; N, 6.96. Found: C, 54.20; H, 5.64; N, 6.84.

[P(OEP)(F)(OCH_3)]$^+$$PF_6^-$ (6h-PF_6). A solution of [P(OEP)(F)-(OH)]$^+$Cl$^-$ (27.8 mg, 43.8 μmol) in dichloromethane (30 mL) was washed with aqueous NaOH (pH 11, 80 mL) and the solvent then evaporated. MeI (1.0 mL, 16 mmol) and dichloromethane (10 mL) were added to the residue, and the solution was stirred for 40 h at room temperature. After evaporation of the solvent, the residue was chromatographed (benzene/methyl acetate/methanol; 15:15:1) to give [P(OEP)(F)(OCH_3)]$^+$$OH^-$. Counteranion exchange with potassium hexafluorophosphate gave [P(OEP)(F)(OCH_3)]$^+$$PF_6^-$ (17.2 mg, 52%): mp 148−152 °C (dichloromethane/*n*-hexane; 1:1). ^{1}H NMR ($CDCl_3$) δ −2.19 (d, 3 H, J = 24.9 Hz), 1.84 (t, 24 H, J = 7.3 Hz), 3.95 (bm, 16 H), 9.44 (s, 4 H). ^{31}P NMR ($CDCl_3$) δ −183.6 (d, J = 808 Hz), −143.7 (sept, J = 712 Hz). ^{19}F NMR ($CDCl_3$) δ −74.2 (d, 6 F, J = 712 Hz), −35.5 (d, 1 F, J = 808 Hz). Anal. Calcd for $C_{37}H_{47}N_4OP_2F_7$: C, 58.57; H, 6.24; N, 7.38. Found: C, 58.63; H, 6.13; N, 7.44.

Preparation of [P(OEP)($R)_2$]$^+$$PF_6^-$. Trialkylaluminum in *n*-hexane (5.07 mmol) was added to a solution of [P(OEP)($Cl)_2$]$^+$Cl$^-$ (678 mg, 1.07 mmol) in dichloromethane (15 mL) under nitrogen at room temperature. The mixture was heated under reflux for 24 h, after which it was treated with cold water and then filtered through Celite. Extraction, removal of the solvent in vacuo, and purification by chromatography (benzene/methyl acetate/methanol; 15:15:1) gave

$[P(OEP)(R)_2]^+Cl^-$. Counteranion exchange with potassium hexafluorophosphate was carried out.

$[P(OEP)(CH_3)_2]^+PF_6^-$ (11a-PF_6). 24% Yield; mp 240−245 °C (dichloromethane/ether; 1:1). UV−vis (CH_2Cl_2) λ ($\epsilon \times 10^{-3}$) 367 (35.7), 407 (50.7), 429 (253), 556 (13.9), 595 (8.63). ^{1}H NMR ($CDCl_3$) δ −6.21 (d, 6 H, J = 16.9 Hz), 1.98 (t, 24 H, J = 7.7 Hz), 4.15 (q, 16 H, J = 7.7 Hz), 10.04 (s, 4 H). ^{31}P NMR ($CDCl_3$) δ −190.9 (s), −143.8 (sept, J = 713 Hz). Anal. Calcd for $C_{38}H_{50}N_4P_2F_6$: C, 61.78; H, 6.82; N, 7.58. Found: C, 61.50; H, 6.59; N, 7.64.

$[P(OEP)(CH_2CH_3)_2]^+PF_6^-$ (11b-PF_6). 20% Yield; mp 267−269 °C (dichloromethane/*n*-hexane; 1:1). UV−vis (CH_2Cl_2) λ ($\epsilon \times 10^{-3}$) 365 (41.5), 408 (52.3), 430 (236), 554 (15.5), 594 (6.33). ^{1}H NMR ($CDCl_3$) δ −6.41 (dq, 4 H, J = 14.3, 7.2 Hz), −5.04 (dt, 6 H, J = 37.4, 7.2 Hz), 1.96 (t, 24 H, J = 7.6 Hz), 4.19 (q, 16 H, J = 7.6 Hz), 10.23 (s, 4 H). ^{31}P NMR ($CDCl_3$) δ −159.5 (s), −143.8 (sept, J = 713 Hz). ^{13}C NMR ($CDCl_3$) δ 5.07 (d, J = 9.0 Hz), 18.41 (d, J = 19.6 Hz), 45.27 (d, J = 235 Hz), 95.62 (d, J = 3.7 Hz), 140.1 (s), 143.6 (s). Anal. Calcd for $C_{40}H_{54}N_4P_2F_6$: C, 63.48; H, 7.19; N, 7.41. Found: C, 63.32; H, 7.18; N, 7.42.

Preparation of $[P(OEP)(CH_3)(R)]^+PF_6^-$. PCl_3 (0.1 mL, 1.2 mmol) was added to a solution of $[P(OEP)(R)(OH)]^+Cl^-$ (98.7 mg, 156 μmol) in dichloromethane (5 mL) and the solution was stirred for 7 days at room temperature. After evaporation of the solvent, dichloromethane (10 mL) and trimethylaluminum (0.909 mol/L solution in *n*-hexane, 1.20 mL, 1.1 mmol) were added under nitrogen at room temperature. The mixture was stirred for 1 h at room temperature after which it was treated with cold water and then filtered through Celite. Extraction, removal of the solvent in vacuo, and purification by chromatography (benzene/methyl acetate/methanol; 15:15:1) gave $[P(OEP)(CH_3)(R)]^+Cl^-$. Counteranion exchange with potassium hexafluorophosphate was carried out.

$[P(OEP)(CH_3)(CH_2CH_3)]^+PF_6^-$ (11c-PF_6). 11.5% Yield; mp 240−244 °C (dichloromethane/*n*-hexane; 1:1). UV−vis (CH_2Cl_2) λ ($\epsilon \times 10^{-3}$) 365 (38.9), 408 (51.4), 430 (253), 556 (14.7), 595 (7.57). ^{1}H NMR ($CDCl_3$) δ −6.31 (d, 3 H, J = 16.9 Hz), −6.25 (dq, 2 H, J = 14.7, 7.3 Hz), −4.95 (dt, 3 H, J = 45.5, 7.3 Hz), 1.98 (t, 24 H, J = 7.6 Hz), 4.18 (q, 16 H, J = 7.6 Hz), 10.13 (s 4 H). ^{31}P NMR ($CDCl_3$) δ −176.1 (s), −143.8 (sept, J = 713 Hz). Anal. Calcd for $C_{39}H_{52}N_4P_2F_6 \cdot 0.5CH_2Cl_2$: C, 59.65; H, 6.72; N, 7.05. Found: C, 59.94; H, 6.73; N, 7.08.

$[P(OEP)(C_6H_5)(CH_3)]^+PF_6^-$ (11d-PF_6). 59.8% Yield; mp 235−238 °C (dichloromethane/ethyl acetate/*n*-hexane; 1:1:1):. UV−vis (CH_2Cl_2) λ ($\epsilon \times 10^{-3}$) 364 (37.4), 409 (54.2), 431 (280), 557 (14.4), 598 (11.8). ^{1}H NMR ($CDCl_3$) δ −5.72 (d, 3 H, J = 16.1 Hz), −0.05 (dd, 2 H, J = 26.4, 8.1 Hz), 1.87 (t, 24 H, J = 7.2 Hz), 4.03 (dq, 8 H, J = 14.5, 7.2 Hz), 4.07 (dq, 8 H, J = 14.5, 7.2 Hz), 4.62 (ddd, 2 H, J = 7.6, 7.6, 7.6 Hz), 5.33 (dt, 1 H, J = 4.4, 7.6 Hz), 9.72 (s, 4 H). ^{31}P NMR ($CDCl_3$) δ −196.8 (s), −143.7 (sept, J = 713 Hz). Anal. Calcd for $C_{43}H_{52}N_4P_2F_6$: C, 64.49; H, 6.55; N, 7.00. Found: C, 64.45; H, 6.61; N, 6.94.

$[P(OEP)(C_6H_5)(CH_2CH_3)]^+PF_6^-$ (11e-PF_6). 23% Yield; mp >300 °C (dichloromethane/ethyl acetate/*n*-heptane; 1:1:1). UV−vis (CH_2Cl_2) λ ($\epsilon \times 10^{-3}$) 366 (39.7), 411 (56.9), 432 (266), 559 (14.5), 598 (10.9). ^{1}H NMR ($CDCl_3$) δ −5.68 (dq, 2 H, J = 13.7, 7.2 Hz), −4.58 (dt, 3 H, J = 43.3, 7.2 Hz), −0.10 (dd, 2 H, J = 25.7, 7.8 Hz), 1.87 (t, 24 H, J = 7.4 Hz), 4.06 (dq, 8 H, J = 14.8, 7.4 Hz), 4.10 (dq, 8 H, J = 14.8, 7.4 Hz), 4.60 (ddd, 2H, J = 7.8, 7.8, 7.8 Hz), 5.31 (dt, 1 H, J = 4.4, 7.8 Hz), 9.78 (s, 4 H). ^{31}P NMR ($CDCl_3$) δ −184.0 (s), −143.7 (sept, J = 713 Hz). ^{13}C NMR ($CDCl_3$) δ 5.81 (d, J = 12.9 Hz), 18.13 (d, J = 19.7 Hz), 42.92 (d, J = 237 Hz), 94.92 (s), 139.1 (s), 144.7 (s). Anal. Calcd for $C_{44}H_{54}N_4P_2F_6$: C, 64.85; H, 6.68; N, 6.88. Found: C, 64.54; H, 6.81; N, 6.90.

X-ray Structure Determination. Crystal data of the structure determinations are given in Tables 1a−1c (and Table 7 in Supporting Information). Crystals suitable for X-ray structure determination were mounted on a Mac Science MXC3 diffractometer and irradiated with graphite-monochromated Mo Kα radiation (λ = 0.71073 Å) or Cu Kα radiation (λ = 1.54178 Å) for data collection. Lattice parameters were determined by least-squares fitting of 31 reflections for $[P(OEP)(Cl)_2]^+PF_6^-$ (**1**-PF_6) with 31° < 2θ < 35°, of 27 reflections for $[P(OEP)(CH_2CH_3)(OH)]^+ClO_4^-$ (**2b**-ClO_4) with 31° < 2θ < 35°, of 31 reflections for $[P(OEP)(C_6H_5)(OH)]^+PF_6^-$ (**2c**-PF_6) with 30° < 2θ < 35°, of 29 reflections for $[P(OEP)(F)(OH)]^+ClO_4^-$ (**2d**-ClO_4) with 56° < 2θ < 61°, of 26 reflections for $[P(OEP)(CH_2CH_3)(=O)]$ (**3b**) with 12° < 2θ < 27°, of 29 reflections for $[P(OEP)(C_6H_5)(OCH_2CH_2CH_3)]^+ClO_4^-$ (**6f**-ClO_4) with 56° < 2θ < 60°, of 24 reflections for $[P(OEP)(CH_2CH_3)(N(CH_2CH_3)_2)]^+ClO_4^-$ (**7a**-ClO_4) with 19° < 2θ < 30°, of 31 reflections for $[P(OEP)(CH_3)(F)]^+PF_6^-$ (**9a**-PF_6) with 47° < 2θ < 61°, of 23 reflections for $[P(OEP)(C_6H_5)(F)]^+PF_6^-$ (**9c**-PF_6) with 25° < 2θ < 31°, of 31 reflections for $[P(OEP)(CH_3)_2]^+PF_6^-$ (**11a**-PF_6) with 24° < 2θ < 32°, and of 29 reflections for $[P(OEP)(CH_2CH_3)_2]^+PF_6^-$ (**11b**-PF_6) with 30° < 2θ < 35°. Data were collected by use of the ω scan mode. The structures were solved using the SIR-92 program in teXsan (Rigaku) package (ver 1.11).[60] Refinement on F was carried out by full-matrix least-squares. No absorption correction was made. All non-hydrogen atoms were refined with anisotropic thermal parameters. Hydrogen atoms were included in the refinement on calculated positions (C−H = 1.0 Å) riding on their carrier atoms with isotropic thermal parameters except those of water in $[P(OEP)(Cl)_2]^+PF_6^-$ (**1**-PF_6) and of OH groups in $[P(OEP)(CH_2CH_3)(OH)]^+ClO_4^-$ (**2b**-ClO_4) and $[P(OEP)(C_6H_5)(OH)]^+PF_6^-$ (**2c**-PF_6) which could be found on a difference Fourier map and these coordinates were included in the refinement. The dichloromethane solvent which was found incorporated in $[P(OEP)(CH_3)_2]^+PF_6^-$ (**11a**-PF_6) and **2c**-PF_6 was disordered; these were treated by refining the occupancies of the group in two possible configurations in **11a**-PF_6 or three possible configurations in **2c**-PF_6. The solvent ethyl acetate in **2b**-ClO_4 was disordered but only part of the structure could be included in the refinement on fixed positions. All computations were carried out on an SGI O_2 computer using the teXsan program.[60]

Results and Discussion

Synthesis of Phosphorus Octaethylporphyrins. The insertion of phosphorus into octaethylporphyrin was accomplished by reaction of $(OEP)H_2$ with PCl_3 in the presence of 2,6-dimethylpyridine, which has been shown to be superior to pyridine for insertion of antimony[29] and arsenic[31,32] into either free base octaethyl- or tetraphenylporphyrins. The main product was $[P(OEP)(Cl)_2]^+Cl^-$ (**1**-Cl). Similarly, the reaction of $RPCl_2$ with $(OEP)H_2$ gave $[P(OEP)(R)(Cl)]^+Cl^-$ (**4**-Cl) in the presence of 2,6-dimethylpyridine, although the corresponding reaction of $RSbCl_2$ with $(OEP)H_2$ gave (OEP)SbCl.[29] The mechanism for oxidation of the phosphorus(III) to the phosphorus(V) porphyrin is not clear. However, it probably involves oxidation of initially formed P(OEP)(R) by trace oxygen in Ar, and the oxidized P(V) species is converted to $[P(OEP)(R)(Cl)]^+Cl^-$ by excess PCl_3. $[P(OEP)(R)(OH)]^+Cl^-$ could be isolated by treating a solution of the mixture in dichloromethane with aq dilute HCl (pH ca. 3). P(OEP)(R)(O) (**3**) could also be isolated by treating the mixture of $[P(OEP)(R)(OH)]^+Cl^-$ and P(OEP)(R)(O) with aq dilute Na_2CO_3 (pH ca. 11) (Scheme 1). These mono-alkylated compounds, **2** and **3**, are stable to atmospheric moisture and chromatographic treatment.

The hydroxyl group of $[P(OEP)(R)(OH)]^+Cl^-$ (**2**) could be converted to the corresponding chloride, giving $[P(OEP)(R)(Cl)]^+Cl^-$ (**4**) by treatment with PCl_3. However, the conversion was sluggish at room temperature and the formation of $[P(OEP)(R)(OPCl_2)]^+Cl^-$ (**5**) was occasionally observed as an intermediate. Alcohols reacted with the mixture of **4** and **5** to form the corresponding alkoxy derivatives, $[P(OEP)(R)(OR')]^+Cl^-$ (**6**), in good yields. *tert*-BuOH did not react with the mixture of $[P(OEP)(R)(Cl)]^+Cl^-$ and $[P(OEP)(R)(OPCl_2)]^+Cl^-$, probably because of steric hindrance. Amines also reacted with the mixture but the yield of the corresponding amino derivatives were generally poor. $[P(OEP)(CH_2CH_3)(N(CH_2CH_3)_2)]^+ClO_4^-$ (**7a**-ClO_4) and $[P(OEP)(CH_2CH_3)(NH(CH_2CH_2CH_2CH_3))]^+ClO_4^-$ (**7b**-ClO_4) were obtained in 12% and 12% yields, respectively, after counteranion exchange (Scheme 2).

(60) The program is available from Rigaku Co.

Table 1. Crystallographic Data for $[P(OEP)(CH_2CH_3)(OH)]^+ClO_4^-$ (**2b**-ClO_4), $P(OEP)(F)(OH)]^+ClO_4^-$ (**2d**-PF_6), $[P(OEP)(CH_2CH_3)(O)]$ (**3b**), $[P(OEP)(C_6H_5)(On\text{-}Pr)]^+ClO_4^-$ (**6f**-ClO_4), $[P(OEP)(C_6H_5)(F)]^+PF_6^-$ (**9c**-PF_6), $[P(OEP)(CH_3)_2]^+PF_6^-$ (**11a**-PF_6), and $[P(OEP)(CH_2CH_3)_2]^+PF_6^-$ (**11b**-PF_6)

molecule	$[P(OEP)(CH_2CH_3)(OH)]^+ClO_4^-$(**2b**-$ClO_4$)	$[P(OEP)(F)(OH)]^+ ClO_4^-$(**2d**-$ClO_4$)	$[P(OEP)(CH_2CH_3)(O)]$(**3b**)
formula	$C_{38}H_{50}N_4O_5PCl + 0.5CH_3CO_2Et$	$C_{36}H_{45}N_4FClO_5P$	$C_{38}H_{49}N_4OP + H_2O$
mol wt	753.3	699.2	626.8
cryst syst	triclinic	triclinic	monoclinic
space group	*P*1	*P*1	$P2_1$
cryst dimens, mm	1.00 × 0.90 × 0.45	0.80 × 0.30 × 0.07	0.35 × 0.25 × 0.15
color	violet	violet	violet
habit	plate	plate	plate
a, Å	11.612(4)	11.626(2)	10.990(3)
b, Å	14.250(6)	12.863(3)	15.570(4)
c, Å	14.417(7)	13.373(3)	10.251(3)
α, deg	67.47(4)	110.06(2)	90
β, deg	69.71(3)	105.60(2)	98.05(3)
γ, deg	70.51(3)	95.09(2)	90
V, Å^3	2010(1)	1772.7(8)	1736.8(8)
Z	2	2	2
D_{calc}, g cm^{-3}	1.24	1.31	1.20
abs coeff, cm^{-1}	1.41	17.08	0.81
F(000)	804	740	676
radiation: *λ*, Å	Mo Kα, 0.71073	Cu Kα, 1.54178	Mo Kα, 0.71073
temp, °C	23 ± 1	23 ± 1	23 ± 1
2*θ* max, deg	55	130	50
scan rate, deg/min	6.0	2.5	1.0
linear decay, %	3	-	-
data collected	±*h*,+*k*,±*l*	-*h*,±*k*,±*l*	±*h*,+*k*,+*l*
total data collcd, unique, obsd	9719, 9245, 5767 ($I > 3\sigma(I)$)	6311, 5921, 4495($I > 3\sigma(I)$)	3412, 3165, 2184 ($I > 1\sigma(I)$)
no of params refined	451	433	406
R, R_w	0.072, 0.115[a]	0.068, 0.111[a]	0.074, 0.110[a]
goodness of fit (obs)	1.26	1.34	1.16
max shift in final cycle	0.070	0.021	0.002
final diff map, max, e/Å^3	0.60	0.42	0.37

molecule	$[P(OEP)(C_6H_5)(On\text{-}Pr)]^+ClO_4^-$(**6f**-$ClO_4$)	$[P(OEP)(C_6H_5)(F)]^+PF_6^-$(**9c**-$PF_6$)	$[P(OEP)(CH_3)_2]^+ PF_6^-$(**11a**-$PF_6$)
formula	$C_{45}H_{56}N_4O_5ClP$	$C_{42}H_{50}N_4P_2F_7$	$C_{38}H_{50}N_4F_6P_2 + CH_2Cl_2$
mol wt	799.4	805.8	823.7
cryst syst	orthorhombic	monoclinic	monoclinic
space group	$Pna2_1$	*C*2/*c*	$P2_1/m$
cryst dimens, mm	0.90 × 0.40 × 0.20	0.40 × 0.20 × 0.06	0.55 × 0.25 × 0.15
color	violet	violet	violet
habit	plate	plate	plate
a, Å	21.323(4)	28.826(7)	11.584(3)
b, Å	12.523(2)	15.867(3)	18.202)3)
c, Å	16.406(4)	18.145(4)	9.600(2)
α, deg	90	90	90
β, deg	90	98.69(2)	100.94(1)
γ, deg	90	90	90
V, Å^3	4381(2)	8203(3)	1987.2(5)
Z	4	8	2
D_{calc}, g cm^{-3}	1.21	1.31	1.38
abs coeff, cm^{-1}	14.04	13.69	2.57
F(000)	1704	3447	864
radiation; *λ*, Å	Cu Kα, 1.54178	Cu Kα, 1.54178	Mo Kα, 0.71073
temp, °C	23 ± 1	23 ± 1	23 ± 1
2*θ* max, deg	130	100	50
scan rate, deg/min	2.0	1.0	3.0
linear decay, %	-	-	-
data collected	+*h*,+*k*,+*l*	±*h*,+*k*,+*l*	±*h*,−*k*,+*l*
total data collcd, unique, obsd	4148, 3793, 3260($I > 3\sigma(I)$)	7485, 6884, 5588($I > 3\sigma(I)$)	3918, 3642, 1825($I > 4\sigma(I)$)
no of params refined	505	496	268
R, R_w,	0.068, 0.095,	0.067, 0.104[a]	0.085, 0.133[a]
goodness of fit (obs)	1.07	1.02	1.43
max shift in final cycle	0.013	0.002	0.009
final diff map, max, e/Å^3	0.63	0.28	0.95

molecule	$[P(OEP)(CH_2CH_3)_2]^+PF_6^-$(**11b**-$PF_6$)	molecule	$[P(OEP)(CH_2CH_3)_2]^+PF6$-(**11b**-$PF_6$)
formula	$C_{40}H_{54}N_4F_6P_2$	abs coeff, cm^{-1}	1.92
mol wt	766.9	F(000)	812
cryst syst	triclinic	radiation; *λ*, Å	Mo Kα, 0.71073
space group	*P*1	temp, °C	23 ± 1
cryst dimens, mm	0.90 × 0.75 × 0.15	2*θ* max, deg	50
color	violet	scan rate, deg/min	5.0
habit	plate	linear decay,%	3
a, Å	9.769(4)	data collected	±*h*,±*k*,+1
b, Å	10.863(3)	total data collcd, unique, obsd	7333, 7052, 4933($I > 3\sigma(I)$)
c, Å	21.26(1)	no of params refined	490
α, deg	87.73(4)	*R*, R_w,	0.058, 0.099[a]
β, deg	84.59(4)	goodness of fit (obs)	1.39
γ, deg	63.30(3)	max shift in final cycle	0.007
V, Å^3	2006(1)	final diff map, max, e/Å^3	0.26
Z	2		
D_{calc}, g cm^{-3}	1.27		

[a] Function mimimized was sum $[w(|Fo|^2 - |Fc|^2)^2]$ which $w = 1.0/\sum|Fo|^2$ which $w = 1.0/\sum|Fo|^2 + x\ |Fo|^2$, $x = 0.00664$ (**2b**-ClO_4), 0.00601 (**2d**-ClO_4), and 0.00436 (**3b**). [b] Function mimimized was sum $[w(|Fo|^2 - |Fc|^2)^2]$ which $w = 1.0/\sum|Fo|^2$ which $w = 1.0/\sum|Fo|^2 + x\ |Fo|^2$, $x = 0.00664$ (**6f**-ClO_4), 0.0970 (**9c**-PF_6), and 0.0774 (**11a**-PF_6). [c] Function mimimized was sum $[w(|Fo|^2 - |Fc|^2)^2]$ which $w = 1.0/\sum|Fo|^2$ which $w = 1.0/\sum|Fo|^2 + x\ |Fo|^2$, $x = 0.00410$ (**11b**-PF_6).

Scheme 1

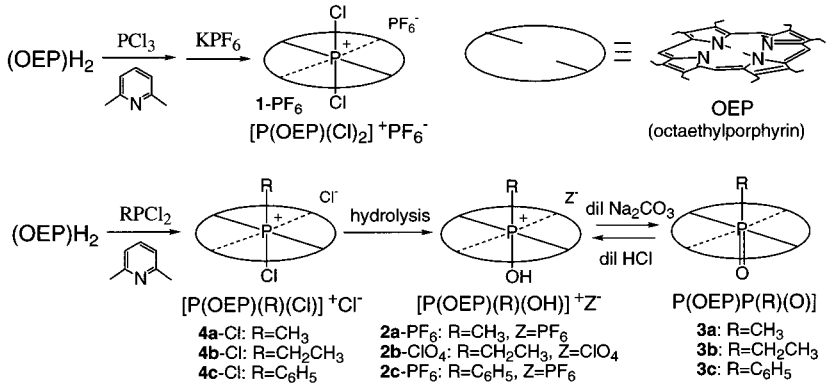

Scheme 2

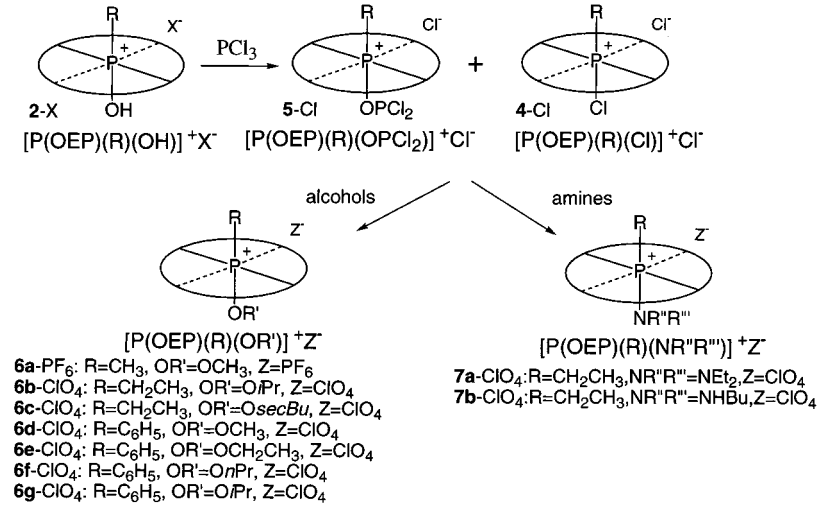

Scheme 3

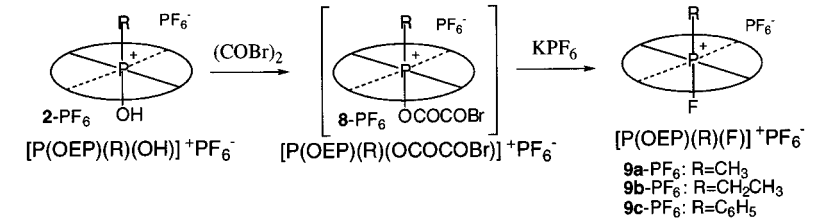

A fluoride anion could be introduced from the PF_6^- counteranion of $[P(OEP)(R)(OH)]^+PF_6^-$ (**2**-PF_6) via conversion of the OH group to the corresponding $[P(OEP)(R)(OCOCOBr)]^+PF_6^-$ (**8**-PF_6) by the reaction of oxalyl bromide (Scheme 3).[18,30,33] In the case of $[P(OEP)(CH_3)(OH)]^+PF_6^-$ and $[P(OEP)(CH_2CH_3)(OH)]^+PF_6^-$, the conversion took place smoothly to give $[P(OEP)(CH_3)(F)]^+PF_6^-$ (**9a**-PF_6) and $[P(OEP)(CH_2CH_3)(F)]^+PF_6^-$ (**9b**-PF_6) in 42% and 21% yield, respectively, after counteranion exchange. However, for $[P(OEP)(C_6H_5)(OH)]^+PF_6^-$, solvents such as *tert*-BuOH and acetonitrile were necessary to accelerate the conversion to $[P(OEP)(C_6H_5)(F)]^+PF_6^-$ (**9c**-PF_6) (Scheme 3). The mechanism of fluorination is unclear, but these coordinating and polar solvents were previously found useful for fluorination to give $[(TPP)Sb(CH_3)(F)]^+PF_6^-$ from $[(TPP)Sb(CH_3)(OH)]^+PF_6^-$.[18]

In the case of $[P(OEP)(OH)_2]^+PF_6^-$ (**10**-PF_6), only monofluorinated $[P(OEP)(F)(OH)]^+ClO_4^-$ (**2d**-ClO_4) was obtained in 53% yield after treatment with oxalyl bromide and counteranion exchange. P(OEP)(F)(O) (**3d**) could be prepared quantitatively by treating $[P(OEP)(F)(OH)]^+ClO_4^-$ (**2d**-ClO_4) with aq dilute NaOH (pH ca. 11) or 1,8-diazabicyclo[5.4.0]undec-7-ene (DBU), but [P(OEP)(F)(O)] (**3d**) was not stable after prolonged standing. A conversion of the hydroxyl group of $[P(OEP)(F)(OH)]^+ClO_4^-$ to the corresponding chloride $[P(OEP)(F)(Cl)]^+Cl^-$ (**4d**-Cl) was very sluggish by treatment with PCl_3 and PCl_5 was necessary in order to carry out the conversion to **4d**-Cl. $[P(OEP)(F)(Cl)]^+Cl^-$, once formed, was found to be stable even toward chromatographic treatment and did not react with MeOH, even under reflux for 3 days. $[P(OEP)(F)(OCH_3)]^+PF_6^-$ (**6h**-PF_6) was obtained by reaction of P(OEP)(F)(O) with CH_3I in 52% yield after counteranion exchange (Scheme 4).

The trialkylaluminum method, which was developed for introduction of alkyl groups into antimony octaethylporphyrins,[29] also worked for the phosphorus octaethylporphyrins. $[P(OEP)(CH_3)_2]^+PF_6^-$ (**11a**-PF_6) and $[P(OEP)(CH_2CH_3)_2]^+PF_6^-$ (**11b**-PF_6) were obtained in 24% and 20% yield, respectively, by the reaction of $[P(OEP)(Cl)_2]^+Cl^-$ (**1**-Cl) with R_3Al (R═CH_3, CH_2CH_3) followed by counteranion exchange (Scheme 5). Unsymmetrical dialkylated compounds such as $[P(OEP)(CH_3)(CH_2$-

Scheme 4

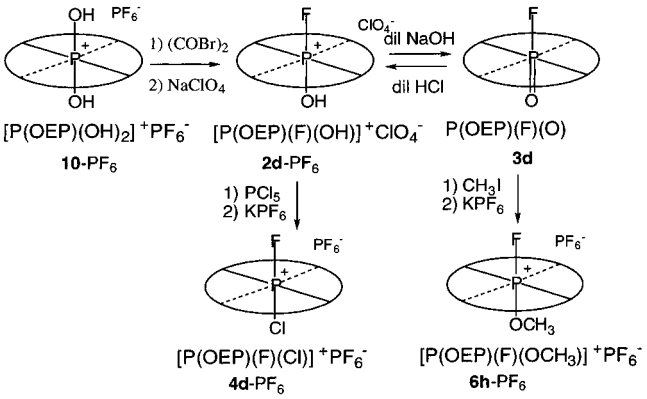

Scheme 5

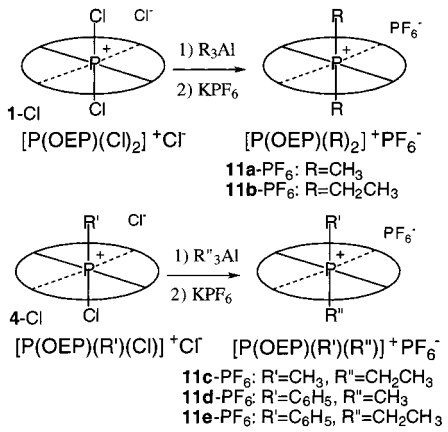

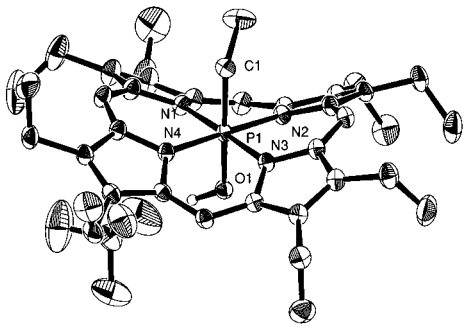

Figure 1. ORTEP diagram (30% probability ellipsoids) for $[P(OEP)(CH_2CH_3)(OH)]^+ClO_4^-$ (**2b**-ClO_4).

$CH_3)]^+PF_6^-$ (**11c**-PF_6), $[P(OEP)(C_6H_5)(CH_3)]^+PF_6^-$ (**11d**-PF_6), and $[P(OEP)(C_6H_5)(CH_2CH_3)]^+PF_6^-$ (**11e**-PF_6) could be prepared in 12%, 60%, and 23% yield, respectively, by the reaction of $[P(OEP)(CH_3)(Cl)]^+Cl^-$ or $[P(OEP)(C_6H_5)(Cl)]^+Cl^-$ with trimethylaluminum or triethylaluminum (Scheme 5).

X-ray Crystallographic Analysis. Crystals suitable for X-ray analysis for the following eleven porphyrins were obtained: **1**-PF_6, **2b**-ClO_4, **2c**-PF_6, **2d**-ClO_4, **3b**, **6f**-ClO_4, **7a**-ClO_4, **9a**-PF_6, **9c**-PF_6, **11a**-PF_6, and **11b**-PF_6. Solvents of recrystallization were found incorporated in the crystal lattice in **2b**-ClO_4 (ethyl acetetate, population 0.5), **2c**-PF_6, **9a**-PF_6, and **11a**-PF_6 (dichloromethane, population 1.0). Figures 1−7 show the ORTEP drawings of **2b**-ClO_4, **2d**-ClO_4, **3b**, **6f**-ClO_4, **9c**-PF_6, **11a**-PF_6, and **11b**-PF_6 (for other compounds, see Supporting Information). The solvents are omitted for clarity (except water in **3b**). In $[P(OEP)(CH_2CH_3)(N(CH_2CH_3)_2)]^+ClO_4^-$ (**7a**-ClO_4), the $P-CH_2-CH_3$ and $P-N(CH_2CH_3)_2$ units could not be differentiated due to the alternately inverse arrangement of the molecule in the crystal, but the structure of the porphyrin core could be definitely determined. The oxygen atom of the axial OH group in **2b**-ClO_4 and **2d**-ClO_4 is hydrogen-bonded with the perchlorate anion (the distance between the hydrogen atom of the OH group and the closest oxygen atom in the perchlorate anion is 1.94 Å in **2b**-ClO_4 and 2.09 Å in **2d**-ClO_4). The oxygen atom in the PO group of **3b** is also hydrogen-bonded with a water molecule (the distance between the oxygen atom of the PO group and the closer hydrogen atom in the water molecule is 1.87 Å). Selected bond distances around the phosphorus atom are listed in Table 2. Each of the geometries about the phosphorus atom is a distorted octahedral. The distance of the PO bond (1.475(7) Å) in $P(OEP)(CH_2CH_3)(O)$ (**3b**) is significantly shorter than the single bond distances seen in $[P(OEP)(CH_2CH_3)(OH)]^+ClO_4^-$ (**2b**-ClO_4) (1.627(2) Å), $[P(OEP)(C_6H_5)(OH)]^+PF_6^-$ (**2c**-PF_6) (1.639(3) Å), $[P(OEP)(F)(OH)]^+ClO_4^-$ (**2d**-ClO_4) (1.618(2) Å), and $[P(OEP)(C_6H_5)(OCH_2CH_2CH_3)]^+ClO_4^-$ (**6f**-ClO_4) (1.649(4) Å). The PO bond in **3b** could be regarded as a double bond since the PO bond distance is almost identical with the reported

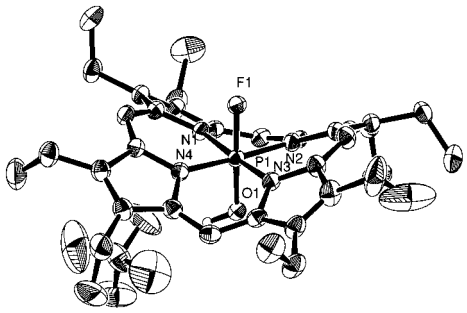

Figure 2. ORTEP diagram (30% probability ellipsoids) for $[P(OEP)(F)(OH)]^+ClO_4^-$ (**2d**-ClO_4).

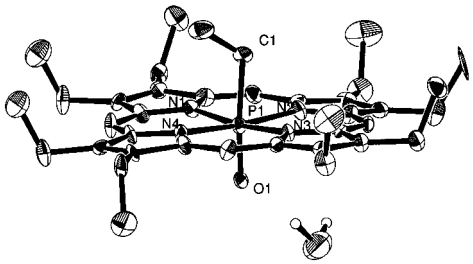

Figure 3. ORTEP diagram (30% probability ellipsoids) for $[P(OEP)(CH_2CH_3)(O)]$ (**3b**).

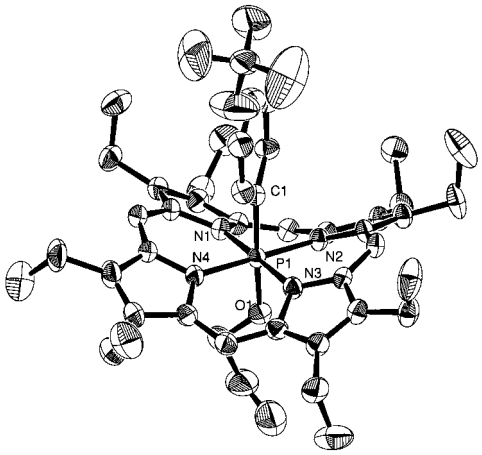

Figure 4. ORTEP diagram (30% probability ellipsoids) for $[P(OEP)(C_6H_5)(OCH_2CH_2CH_3)]^+ClO_4^-$ (**6f**-ClO_4).

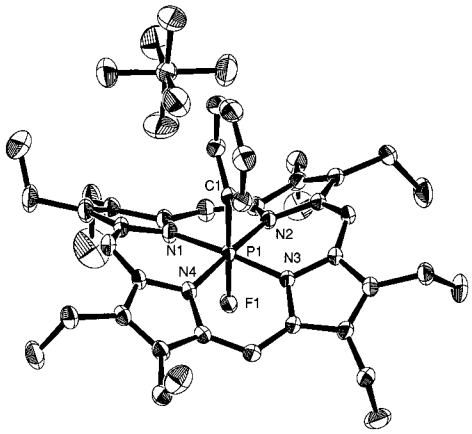

Figure 5. ORTEP diagram (30% probability ellipsoids) for $[P(OEP)(C_6H_5)(F)]^+PF_6^-$ (**9c**-PF_6).

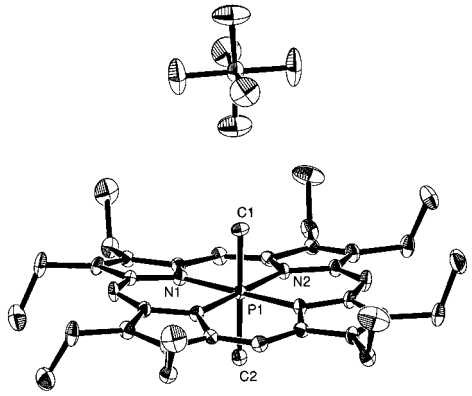

Figure 6. ORTEP diagram (30% probability ellipsoids) for $[P(OEP)(CH_3)_2]^+PF_6^-$ (**11a**-PF_6).

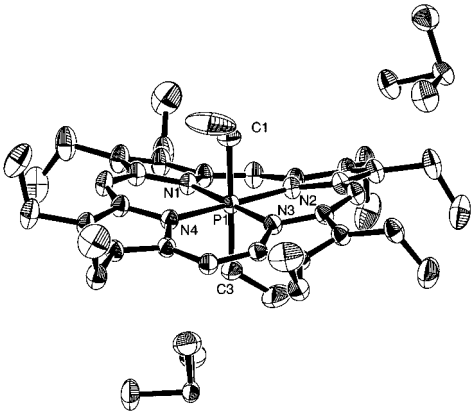

Figure 7. ORTEP diagram (30% probability ellipsoids) for $[P(OEP)(CH_2CH_3)_2]^+PF_6^-$ (**11b**-PF_6).

distance (1.483 Å) of triphenylphosphine oxide.[61] The bonding around the phosphorus atom in **3b** is quite unique and is the first experimental example of a hypervalent 12-P-6 compound bearing a P═O double bond. The only examples of compounds of this type (12-P-6) bearing a P═O double bond are theoretically proposed species, i.e., $F_3P(=O)\bullet 2NH_3$ and $(HO)_3P(=O)\bullet 2NH_3$, concerning the mechanism of associated edge inversion, in which two molecules of ammonia are coordinated with the phosphoryl group.[62] The bonding features in **3b** are analyzed by theoretical calculations in a later section of the paper.

Interestingly, the porphyrin core of **3b** is almost planar. In contrast, **2b-ClO$_4$** is severely ruffled and adopts an S_4 ruffled conformation as is evident from Figures 8 and 9. The figures show the deviations (in units of 0.01 Å) of the skeletal atoms from the mean plane defined by the 24 core atoms of the porphyrin.[63] The large deviation in meso-positions is clearly observed in all compounds (for other compounds, see Supporting Information) except for **3b** and therefore the type of distortion should be regarded as ruffled.[64−67] Recently there have been several reports on ruffled structures of phosphorus(V) tetraphenylporphyrin derivatives[2−6] but no systematic study as to the electronic effect of the axial ligands on the degree of ruffling of the porphyrin core has been carried out. To elucidate relationships betweeen the degree of ruffling of the porphyrin core and the nature of the axial ligands, bond distances of the P-axial atom, average P−N bond distance, distance of the P atom from the plane of the four nitrogen atoms (Δ4N), and the degree of ruffling of the core (Δr), which was calculated as the square root of the sum of square of the deviation of each atom from the mean plane,[63] are summarized in Table 2. The table lists the compounds in the order of degree of ruffling based on Δr. **2d**-ClO_4 is the most ruffled and is placed as the first entry of the table. The order is as follows: **2d**-ClO_4 (axial ligands: F, OH. $\Delta r = 0.540$) > **1**-PF_6 (Cl, Cl. 0.510) > **9c**-PF_6 (C_6H_5, F. 0.497) ∼ **9a**-PF_6 (CH_3, F. 0.495) ∼ **6f**-ClO_4 (C_6H_5, $OCH_2CH_2CH_3$. 0.494) > **2c**-PF_6 (C_6H_5, OH. 0.485) > **2b**-ClO_4 (CH_2CH_3, OH. 0.467) > **7a**-ClO_4 (CH_2CH_3, $N(CH_2CH_3)_2$. 0.381) > **11b**-PF_6 (CH_2CH_3, CH_2CH_3. 0.264) > **11a**-PF_6 (CH_3, CH_3. 0.123) > **3b** (CH_2CH_3, O^-. 0.072). In summary, as the axial ligand becomes more electronegative, the degree of ruffling becomes greater and the average P−N bond distance becomes shorter. Therefore, the electronic effect of the axial substituents plays a major role in determining the degree of ruffling and the average P−N bond distance. The steric effect of the substituents plays some role since the degree of ruffling is greater in **11b**-PF_6 than in **11a**-PF_6. Among the series, **3b** is placed on the right side of the table as the last entry (the degree of ruffling is the smallest and the avegrage P−N bond distance is the longest), and the oxygen atom in **3b** should be more electron-donating than any axial ligand bonded with carbon.

It is interesting to note that the phosphorus atom in $[P(OEP)(F)(OH)]^+ClO_4^-$ (**2d**-ClO_4) lies at 0.056 Å out-of-plane of the four nitrogens (Δ4N) toward the oxygen atom. The degree of deviation of the central phosphorus atom from the mean plane of the four nitrogen atoms (Δ4N) becomes larger as the difference of electonegativity between the two axial groups becomes larger {**3b** (axial ligands: O^-, CH_2CH_3. $\Delta 4N = 0.114$) > **9c**-PF_6 (C_6H_5, F. 0.076) ∼ **9a**-PF_6 (CH_3, F. 0.071) > **2d**-ClO_4 (OH, F. 0.056) > **2b**-ClO_4 (CH_2CH_3, OH. 0.020) ∼ **2c**-PF_6 (C_6H_5, OH. 0.018) ∼ **6f**-ClO_4 (C_6H_5, $OCH_2CH_2CH_3$. 0.014)}. The deviation of the central atom is always directed toward less electronegative atoms as shown in Table 2. Based on the degree (0.114 Å) of deviation of the central atom and the direction (toward oxygen) in **3b**, it can be concluded that the oxygen atom in **3b** is strongly electron-donating.

^{1}H and ^{31}P NMR of Phosphorus Porphyrins. Selected ^{1}H and ^{31}P NMR data of a series of $[P(OEP)(CH_2CH_3)(X)]^+Z^-$ complexes are shown in Table 3. The ^{31}P NMR chemical shifts

(61) Ruban, G.; Zabel, V. *Crystallogr. Struct. Commun.* **1976**, *5*, 671.
(62) Dixon, D. A.; Arduengo, A. J.; III. *Int. J. Quantum Chem., Symp.* **1988**, *22*, 85.
(63) Sparks, L. D.; Medforth, C. J.; Park. M.-S.; Chamberlain, J. R.; Ondrias, M. R.; Senge, M. O.; Smith, K. M.; Shelnutt, J. A. *J. Am. Chem. Soc.* **1993**, *115*, 7705.
(64) Scheidt, W. R. *Struct. Bonding (Berlin)* **1987**, *64*, 1.
(65) Senge, M. O. *J. Photochem. Photobiol. B: Biol.* **1992**, *16*, 3.
(66) Scheidt, W. R.; Reed, C. A. *Chem. Rev.* **1981**, *81*, 543.
(67) Ravikanth, M.; Chandrashekar, T. K. *Struct. Bonding (Berlin)* **1995**, *82*, 105.

Table 2. Selected Bond Distances and the Degree of Ruffling of Phosphorus(V) Porphyrins

	molecule										
bond distance	**2d**-ClO_4	**1**-PF_6	**9c**-PF_6	**9a**-PF_6	**6f**-ClO_4	**2c**-PF_6	**2b**-ClO_4	**7a**-ClO_4	**11b**-PF_6	**11a**-PF_6	**3b**
P-axial O (Å)	1.618(2)				1.649(4)	1.639(3)	1.627(2)				1.475(7)
P-axial C1 (Å)			1.857(3)	1.84(1)	1.856(5)	1.863(4)	1.874(4)		1.859(4)	1.80(1)	1.88(1)
P-axial C2 (Å)									1.853(4)	1.84(1)	
P-axial F (Å)	1.622(3)		1.618(2)	1.619(6)							
P-axial Cl1 (Å)		2.139(2)									
P-axial Cl2 (Å)		2.140(2)									
P-core N1(Å)	1.836(3)	1.839(6)	1.852(2)	1.863(10)	1.851(5)	1.859(3)	1.886(3)	1.94(1)	1.952(3)	1.967(6)	2.00(1)
P-core N2(Å)	1.826(3)	1.831(6)	1.858(2)	1.841(9)	1.873(4)	1.872(4)	1.870(3)	1.91(1)	1.947(3)	1.976(6)	2.051(10)
P-core N3(Å)	1.833(3)	1.819(6)	1.842(2)	1.832(10)	1.867(5)	1.872(4)	1.879(3)	1.92(1)	1.934(3)		2.01(1)
P-core N4(Å)	1.836(3)	1.836(6)	1.856(2)	1.849(9)	1.871(4)	1.878(4)	1.896(3)	1.90(1)	1.944(3)		1.985(10)
average P−N bond distance (Å)	1.833(3)	1.831(6)	1.852(2)	1.846(10)	1.866(5)	1.870(4)	1.883(3)	1.92(1)	1.944(3)	1.972(6)	2.01(1)
Δr (Å)[a]	0.540	0.510	0.497	0.495	0.494	0.485	0.467	0.381	0.264	0.123	0.072
Δ4N(Å)[b]	0.056 (toward O)	0.000	0.076 (toward C)	0.071 (toward C)	0.014 (toward C)	0.018 (toward C)	0.020 (toward C)		0.000	0.000	0.114 (toward O)

[a] Δr: square root of the sum of square of deviation of each atom from the mean plane of entire 24 core atoms. [b] Δ4N: distance of the P atom from the plane of the four nitrogen atoms.

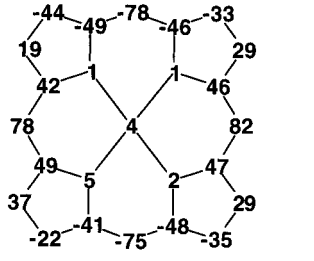

Figure 8. Deviation of each atom from the mean plane ($\Delta r = 0.01$ Å unit) in the molecular structure of $[P(OEP)(CH_2CH_3)(OH)]^+ClO_4^-$ (**2b**-ClO_4).

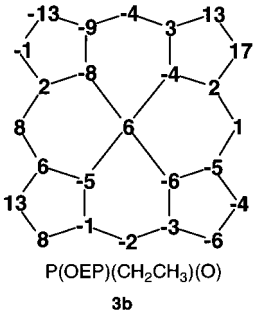

Figure 9. Deviation of each atom from the mean plane ($\Delta r = 0.01$ Å unit) in the molecular structure of $[P(OEP)(CH_2CH_3)(O)]$ (**3b**).

show signals at very high fields (δ −131 ∼ −184) which are consistent with hexacoordinate structures of the central phosphorus atoms.[68] The characteristic axial ethyl signals in the ^{1}H NMR are observed at very high fields (δ (CH_2): −5.32 ∼ −6.41) due to the large ring current effect of the porphyrin nucleus.[18,29−33] The chemical shift is shifted upfield as the electronegativity of the other axial ligand (X) decreases (from left to right in Table 3). This result can be explained by the electronic effect of the axial ligands but, as discussed above, X-ray structural results show that the porphyrin core of $P(OEP)(CH_2CH_3)(O)$ is almost planar as compared to other cationic porphyrin, such as $[P(OEP)(CH_2CH_3)(X)]^+Z^-$ which are severely ruffled. Therefore, the ring current effects of the porphyrin core should be different between compounds with planar structures and those with ruffled structures. In fact, *downfield shifts* are observed for the meso-protons when the electron-donating property of the axial ligands increases from $[P(OEP)(CH_2CH_3)(X)]^+Z^-$ to $P(OEP)(CH_2CH_3)(O)$ (for example, $\delta_{meso} = 9.64$ in **9b**-PF_6 (X = F), 9.72 in **2b**-ClO_4 (X = OH), 10.20 in **3b** (X = O^-)). The downfield shift in **3b** indicates that the ring current effect of the core is larger in the planar **3b** than in the ruffled $[P(OEP)(CH_2CH_3)(X)]^+Z^-$. In contrast, the corresponding arsenic analogue shows *upfield shifts* of the meso-protons upon going from $[As(OEP)(CH_2CH_3)(OH)]^+ClO_4^-$ ($\delta_{meso} = 10.59$) to $As(OEP)(CH_2CH_3)(O)$ ($\delta_{meso} = 10.37$). Since the X-ray structural analysis of $[As(OEP)(CH_3)(OH)]^+ClO_4^-$ showed that the porphyrin core was almost planar,[32] the chemical shift differences in the arsenic porphyrins should originate from the pure electronic effects of the axial ligands. Therefore, the upfield shifts of the meso-protons in the arsenic porphyrins should be due to the electron-donation from the axial oxide without considerable change of ruffling. As for the axial ethyl signals, the ^{1}H NMR chemical shift differences ($\Delta\delta$) between $M(OEP)(CH_2CH_3)(=O)$ and $[M(OEP)(CH_2CH_3)(OH)]^+Z^-$ is much larger in the phosphorus compound than in the corresponding arsenic porphyrins ($\Delta\delta$ $CH_3 = 0.69$ in P, 0.32 in As; $CH_2 = 0.56$ in P, 0.28 in As). The large downfield shifts in phosphorus octaethylporphyrins upon going from $P(OEP)(CH_2CH_3)(O)$ to $[P(OEP)(CH_2CH_3)(X)]^+Z^-$ should be partly due to a decreased ring current effect in severely ruffled $[P(OEP)(CH_2CH_3)(OH)]^+Z^-$ as compared with planar $P(OEP)(CH_2CH_3)(O)$.

UV−Vis Spectra. Characteristic UV−vis spectra have been observed for the high-valent(V) and the low-valent(III) complexes of Group 15 element porphyrins.[69,70] It was concluded that the former porphyrins show normal-type spectra whereas the latter complexes have *p*-type hyper spectra. The electronic absorption spectral data for the series of $[P(OEP)(CH_2CH_3)(X)]^+Y^-$ complexes are summarized in Table 3. These porphyrins exhibit normal type UV−vis spectra with a Soret band in the range of 415−432 nm and two Q-bands in the range of 546−559 and 586−598 nm. The absorption maxima vary with the electron-donating nature of the axial ligand, i.e., the more donating the axial ligand, the longer the wavelength maxima. There is a 12−15 nm red shift for the Soret band of $[P(OEP)(R)_2]^+PF_6^-$ and a 2−8 nm shift for the Q-bands of the compound in relation to $[P(OEP)(F)(OH)]^+ClO_4^-$. Similar shifts

(68) Berger, S.; Braun, S.; Kalinowski, H.-O. In *NMR Spectroscopy of the Non-Metallic Elements*; John Wiley & Sons: Chichester, 1997; Chapter 7, p 700.

(69) Sayer, P.; Gouterman, M.; Connell, C. R. *Acc. Chem. Res.* **1982**, *15*, 73.

(70) Rawlings, D. C.; Davidson, E. R.; Gouterman, M. *Int. J. Quantum Chem.* **1984**, *26*, 251.

Table 3. Selected ^{31}P and ^{1}H NMR Data for $[P(OEP)(CH_2CH_3)(X)]^+Z^-$

molecule	**9b**-PF_6	**2b**-ClO_4	**6b**-ClO_4	**6c**-ClO_4	**7a**-ClO_4	**7b**-ClO_4	**11e**-PF_6	**11c**-PF_6	**11b**-PF_6	**3b**
X	F	OH	O*i*Pr	O*sec*Bu	NEt_2	NHBu	Ph	Me	Et	O^-
^{31}P NMR ($CDCl_3$: δ)	−180.4	−179.8	−169.1	−168.2	−170.4	−174.0	−184.0	−176.1	−159.5	−131.4
^{1}H NMR ($CDCl_3$) (δ_{CH2})	−5.32	−5.70	−6.07	−6.01	−5.92	−5.88	−5.68	−6.25	−6.41	−6.39
(ethyl) (δ_{CH3})	−4.25	−4.52	−4.81	−4.74	−4.67	−4.66	−4.58	−4.95	−5.04	−5.08
(meso-H)	9.64	9.72	9.88	9.98	9.81	9.81	9.78	10.13	10.23	10.20
UV−vis (CH_2Cl_2)	358(23.2)	357(26.9)	357(30.0)	358(30.5)	364(36.5)	364(36.5)	366(39.7)	365(38.9)	365(41.5)	347(27.6)
$\lambda(\epsilon \times 10^{-3})$	415(283)	418(274)	419(237)	419(242)	421(213)	421(213)	432(266)	430(253)	430(236)	417(167)
	549(12.1)	548(13.3)	546(13.2)	546(13.5)	550(13.0)	550(13.0)	559(14.5)	556(14.7)	554(15.5)	539(12.9)
	592(16.4)	590(14.1)	587(13.5)	586(13.7)	589(11.1)	589(11.1)	598(10.9)	595(7.57)	594(6.33)	572(9.68)

have earlier been reported for arsenic,[32] germanium[55] and silicon[58] dihydroxy and dialkyl porphyrins. It is well-known that increasing macrocyclic distortion is accompanied by an increasing red shift of the absorption bands,[71] but such red shift is not observed in the investigated phosphorus porphyrins.

It should be noted that the spectra of the dialkyl compounds, **11b**-PF_6 and **11c**-PF_6, however, show distinct hyper character even though these are higher valent phosphorus(V) compounds, i.e., **11b**-PF_6 and **11c**-PF_6 show an extra Soret band with considerable intensity at 365 nm (ϵ 41,500) and 365 nm (ϵ 38,900), respectively. Since the hyper band has been assigned as a charge-transfer band from the low valent central element to the ligand,[7,70] the electron-donating property of the hypervalent axial bond of the dialkylphosphorus(V) porphyrin ($R-P^+-R$) is thus exemplified.

Nature of the Chemical Bonding of the PO Bond in P(OEP)(CH_2CH_3)(O) (3b). To elucidate the effect of porphyrin substituents on the structures of the core and the properties of compounds, structures of P(OEP)(CH_2CH_3)(O) (**3b**) and P(Por)(CH_2CH_3)(O) (**12b**) (Por: nonsubstituted porphyrin) were optimized by HF/3-21G* level,[72] using the Gaussian 94 program.[73] Since these structures and the electron density population of the two compounds are quite similar, the unsubstituted porphyrin core was used for a detailed analysis in order to save computational time. Thus, the structure of **12b** was further optimized at a high level with nonlocal density functional theory (DFT) using the hybrid Becke 3-Lee−Yang−Parr (B3LYP) exchange-correlation function,[74−77] the basis set employed was 6-31G(d)[78] basis sets for C, N, O, H and 6-311G(2d)[79] for P. The calculated average P−N bond distance is 2.041 Å, which is slightly longer than the experimental value (2.01(1) Å) in **3b**. The calculated PO bond distance (1.492 Å) is also slightly longer than the experimental distance (1.475(7) Å). It is also the case that slightly longer bond distances than experimental ones are obtained by B3LYP calculation in $(CH_3)_3PO$ (calcd 1.484 Å, exp[80] 1.476 Å) and F_3PO (calcd 1.442 Å, exp[81] 1.436 Å). The calculated bond energy of F_3PO (127.4 kcal/mol) is slightly smaller but is still very close to the experimental data (129.5 kcal/mol).[82]

According to natural population analysis,[83,84] the electronic structure of **12b** is $(Por)^{-0.844}(EtPO)^{+0.844}$, indicating that 0.844 electrons are transferred from EtPO to Por. This is mainly caused by an electron transfer from the phosphorus atom. To provide insight into the nature of the PO bond, the electron density $\rho(r)$ and its Laplacian $\nabla^2\rho(r)$ at the bond critical points (r_b) and the elipticity ϵ (a measure of the deviation of the $\rho(r)$ distribution from cylindrical symmetry) were calculated using the Gaussian 94 program[73,85] and analyzed based on *Atoms in Molecules Theory*.[86−96] It has been demonstrated that for ionic bonds, the $\rho(r)$ is depleted in the bond region, reflecting a closed-shell interaction; consequently, $\rho(r_b)$ has a very small value and $\nabla^2\rho(r_b)$ becomes positive. For **12b**, it was calculated that the $\nabla^2\rho(r_b)$ is positive and very large (1.203 e/ao^5), $\rho(r_b)$ has a medium value (0.20 e/ao^3) and the ϵ value (0.002) is close to zero (because of the π-donation of the three lone pairs on O), indicating that the PO bond in **12b** is highly ionic and isotropic. These values are very similar to those of PO bonds in phosphine oxides such as $(CH_3)_3PO$ ($\nabla^2\rho(r) = 1.291$, $\rho(r) = 0.223$, $\epsilon = 0.000$).[97]

To compare the properties of the PO bond in **12b** with those in regular phosphine oxides, the PO bond order (1.792)[98] and bond energy (120.3 kcal/mol) of **12b** were calculated and are found to be smaller than those of CH_3CH_2PO (1.919, 139.1) and $(CH_3)_3PO$ (1.901, 129.0). Thus, the PO bond in **12b** is weaker than in CH_3CH_2PO and $(CH_3)_3PO$. In addition, the structures of P(Por)(CH_2CH_3) and $[P(Por)(CH_2CH_3)(OH)]^+$ were

(71) Barkigia, K. M.; Chantranupong, L.; Smith, K. M. *J. Am. Chem. Soc.* **1988**, *110*, 7566.
(72) Pietro, W. J.; Francl, M. M.; Hehre, W. J.; DeFrees, D. J.; Pople, J. A.; Binkley, J. S. *J. Am. Chem. Soc.* **1982**, *104*, 5039.
(73) Frisch, M. J.; Trucks, G. W.; Schlegel, H. B.; Gill, P. M. W.; Johnson, B. G.; Robb, M. A.; Cheeseman, J. R.; Keith, T.; Petersson, G. A.; Montgomery, J. A.; Raghavachari, K.; Al-Laham, M. A.; Zakrzewski, V. G.; Ortiz, J. V.; Foresman, J. B.; Ciolovski, J.; Stefanov, B. B.; Nanayakkara, A.; Challakombe, M.; Peng, C. Y.; Ayala, P. Y.; Chen, W.; Wong, M. W.; Andres, J. L.; Replogle, E. S.; Gomperts, R.; Martin, R. L.; Fox, D. J.; Binkley, J. S.; DeFrees, D. J.; Baker, J.; Stewart, J. P.; Head-Gordon, C.; Gonzalez, C.; Pople, J. A. *Gaussian 94*; Gaussian, Inc.: Pittsburgh, PA, 1995.
(74) Becke, A. D. *J. Chem. Phys.* **1993**, *98*, 5648.
(75) Becke, A. D. *Phys. Rev.* **1988**, *A38*, 3098.
(76) Perdew, J. P. *Phys. Rev.* **1986**, *B33*, 8822.
(77) Lee, C.; Yang, W.; Parr, R. G. *Phys. Rev.* **1988**, *B37*, 785.
(78) Francl, M. N.; Pietro, W. J.; Hehre, W. J.; Binkley, J. S.; Gordon, M. S.; DeFrees, D. J.; Pople, J. A. *J. Chem. Phys.* **1982**, *77*, 3654.
(79) McLean, A. D.; Chandler, G. S. *J. Chem. Phys.* **1982**, *77*, 3654.
(80) Wilkins, C. J.; Hagen, K.; Hedberg, L.; Shan, Q.; Hedberg, K. *J. Am. Chem. Soc.* **1975**, *97*, 6352.
(81) Reed, A. E.; Weinstock, R. B.; Weinhold, F. *J. Chem. Phys.* **1985**, *83*, 735.
(82) Reed, A. E.; Curtiss, L. A.; Weinhold, F. *Chem. Rev.* **1988**, *88*, 899.
(83) Moritani, T.; Kuchitsu, K.; Morino, Y. *Inorg. Chem.* **1971**, *10*, 344.
(84) Hartley, S. B.; Holmes, W. S.; Jaques, J. K.; Mole, M. F.; McCoubrey, J. C. *Quart. Rev.* **1963**, *17*, 204.
(85) Cioslowski, J.; Nanayakkara, A. *Chem. Phys. Lett.* **1994**, *219*, 151.
(86) Bader, R. F. W. *Atoms in Molecules: a quantum theory*; Clarendon Press: Oxford, 1990.
(87) Bader, R. F. W. *Chem. Rev.* **1991**, *91*, 893.
(88) Bader, R. F. W. *Phys. Chem.* **1998**, *A102*, 7314.
(89) Hernández-Laguna, A.; Sainz-Díaz, C. I.; Smeyers, Y. G.; de Paz, J. L. G.; Gálvez Ruano, E. *J. Phys. Chem.* **1994**, *98*, 1109.
(90) Dobado, J. A.; Molina, J. *J. Phys. Chem.* **1994**, *98*, 1819.
(91) Navarro, J. A. R.; Romero, M. A.; Salas, J. M.; Quiros, M.; El-Bahraoui, J.; Molina, J. *Inorg. Chem.* **1996**, *35*, 7829.
(92) Heinemann, C.; Muller, T.; Apeloig, Y.; Schwarz, H. *J. Am. Chem. Soc.* **1996**, *118*, 2023.
(93) Fan, M. F.; Jia, G. C.; Lin, Z. Y. *J. Am. Chem. Soc.* **1996**, *118*, 9915.
(94) Sainz-Díaz, C. I.; Hernández-Laguna, A.; Smeyers, Y. G. *J. Mol. Struct. (THEOCHEM)* **1997**, *390*, 127.
(95) Dobado, J. A.; Portal, D.; Molina, J. *J. Phys. Chem. A* **1998**, *102*, 778.
(96) El-Bahraoui, J.; Molina, J.; Portal, D. *J. Phys. Chem. A* **1998**, *102*, 2443.
(97) Dobado, J. A.; Martínez-Garcia, H.; Molina, J. M.; Sundberg, M. R. *J. Am. Chem. Soc.* **1998**, *120*, 8461.
(98) Mayer, I. *Int. J. Quantum Chem.* **1986**, *29*, 73; **1986**, *29*, 477.

also optimized by B3LYP. The PO bond distance (1.651 Å) in $[P(Por)(CH_2CH_3)(OH)]^+$ is slightly longer but is consistent with the bond distance in $[P(OEP)(CH_2CH_3)(OH)]^+ClO_4^-$ (**2b**-ClO_4) (1.627(2) Å). The degree of ruffling ($\Delta r = 0.400$) in $[P(Por)(CH_2CH_3)(OH)]^+$ is slightly smaller than in **2b**-ClO_4 (0.462). This difference may be due to the absence of substituents on the porphyrin core since these substituents have been known to affect the degree of distortion of the porphyrin ring.[33,99−103] The PO bond order in $[P(Por)(CH_2CH_3)(OH)]^+$ is calculated to be 1.079, which is significantly smaller than that of **12b** (1.792). Therefore, the π-donation of the three lone pairs on the relatively anionic oxygen in the P^+-O^- bond of **12b** toward the central phosphorus atom is significant and about 24% of the electrons in each lone pairs are transferred to the phosphorus atom. The weaker PO bond in **12b** than in $(CH_3)_3PO$ is due to the smaller π-donation in **12b** because the energy levels (1.62 and 1.63 eV) of orbitals accepting the electrons in the $P(Por)(CH_2CH_3)$ part of **12b** are calculated to be higher than those (1.44 and 1.44 eV) in the $(CH_3)_3P$ part of $(CH_3)_3PO$.

To elucidate the effect of substituents on the properties of the PO bond in the porphyrin series, the structure of P(Por)(F)(O) (**13b**) was optimized by B3LYP together with F_3PO. The PO bond distance (1.486 Å) in **13b** is slightly shorter than that of **12b** (1.492 Å) although the difference is much smaller than that between F_3PO (1.442 Å) and $(CH_3)_3PO$ (1.484 Å). The bond order in **13b** (1.847) is larger than that of **12b** (1.792), but the PO bond energy of **13b** (117.3 kcal/mol) is smaller than that of **12b** (120.3 kcal/mol). Since the energy levels (1.55 and 1.55 eV) of orbitals accepting the electrons in the P(Por)(F) part of **13b** are lower than those (1.62 and 1.63 eV) in the $P(Por)(CH_2CH_3)$ part of **12b**, the π-donation from the lone pairs on the oxygen in the P^+-O^- bond in **13b** toward the central phosphorus atom is more significant than in **12b**, resulting in a shorter PO bond distance and a larger bond order in **13b**. However, the HOMO level (−4.77 eV) of the P(Por)(F) part of **13b** is much lower than that (−4.35 eV) of the $P(Por)(CH_2CH_3)$ part of **12b**. Therefore, the PO bond energy becomes smaller in **13b** than in **12b**. These results are consistent with the data between F_3PO (PO bond distance = 1.442 Å, PO bond order = 2.002, bond energy = 127.4 kcal/mol) and $(CH_3)_3PO$ (PO bond distance = 1.484 Å, PO bond order = 1.901, bond energy = 129.0 kcal/mol). The energy levels of the orbitals accepting electrons (−0.23 eV) and HOMO (−8.69 eV) of the F_3P part of F_3PO are lower than those (+1.44, +1.44 eV (orbitals accepting electrons), −6.03 eV (HOMO)) of the $(CH_3)_3P$ part of $(CH_3)_3PO$.

Electrochemistry. Nine phosphorus derivatives were investigated as to their electrochemistry in PhCN and CH_2Cl_2 containing 0.1 M TBAP as supporting electrolyte. The redox potentials for these compounds are summarized in Table 4 and selected cyclic voltammograms in CH_2Cl_2 are presented in Figure 10. The room-temperature electrochemistry of $[P(OEP)(X)(Y)]^+$ in PhCN or CH_2Cl_2 is dependent upon the nature of the coordinated axial ligand X and Y, as shown in Figure 10.

$[P(OEP)(CH_3)_2]^+$ undergoes two reversible one-electron reductions (labeled as process I and II) at $E_{1/2} = -0.90$ and −1.37 V in CH_2Cl_2. The same electrochemical behavior is observed for $[P(OEP)(CH_3)(OCH_3)]^+$, $[P(OEP)(C_2H_5)(OCH_3)]^+$ and $[P(OEP)(C_6H_5)(OCH_3)]^+$. The first reversible reduction of these porphyrins occurs at potentials which range from −0.70 to −0.90 V while the second reversible reductions are located at $E_{1/2}$ values between −1.27 and −1.37 V in CH_2Cl_2. The

Table 4. Half-Wave Potentials (V vs SCE) of P(V) Octaethylporphyrins in PhCN and CH_2Cl_2 Containing 0.1 M TBAP

solvent	axial ligands		temp (°C)	oxidation	reduction				$\Delta E_{1/2}$
				I	I	II	II′	III	
PhCN	CH_3	CH_3	22	1.41	−0.80	−1.29			2.21
		OCH_3^-	22	1.44	−0.77	−1.28			2.21
	C_2H_5	OCH_3^-	22	1.46	−0.77	−1.28			2.23
	C_6H_5	OCH_3^-	22	1.46	−0.77	−1.29		−1.58	2.23
	CH_3	OH^-	22	1.41	−0.81	−1.28[a]	−1.38[a]	−1.41[a]	2.22
	C_2H_5	OH^-	22	1.42	−0.84	−1.36[a]	−1.46[a]	−1.55[a]	2.26
	C_6H_5	OH^-	22	1.43	−0.82	−1.32[a]		−1.53[a]	2.25
	CH_3	F^-	22	1.40	−0.83[a]	−1.31		−1.60[a]	2.23
	OCH_3^-	F^-	22	1.58	−0.74[a]	−1.31		−1.61[a]	2.32
CH_2Cl_2	CH_3	CH_3	22	1.39	−0.90	−1.37			2.29
		OCH_3^-	22	1.51	−0.81	−1.34			2.32
	C_2H_5	OCH_3^-	22	1.58	−0.78	−1.34			2.36
	C_6H_5	OCH_3^-	22	1.64	−0.70	−1.27			2.34
	CH_3	OH^-	22	1.38	−0.84	−1.33[a]	−1.42[a]	−1.56[a]	2.22
		OH^-	−70	1.37	−0.86	−1.26			2.23
	C_2H_5	OH^-	22	1.35	−0.84	−1.30[a]	−1.43[a]		2.19
		OH^-	−70	1.35	−0.85	−1.27			2.20
	C_6H_5	OH^-	22	1.43	−0.82	−1.33[a]	−1.39[a]	−1.72[a]	2.25
		OH^-	−70	1.39	−0.83	−1.28			2.22
	CH_3	F^-	22	1.54	−0.77[a]	−1.22		−1.75[a]	2.31
		F^-	−70	1.52	−0.78	−1.17			2.30
	OCH_3^-	F^-	22	1.50	−0.80[a]	−1.32		−1.70[a]	2.30
		F^-	−70	1.54	−0.74	−1.15			2.28

[a] E_{pc}, scan rate at 100 mV/s.

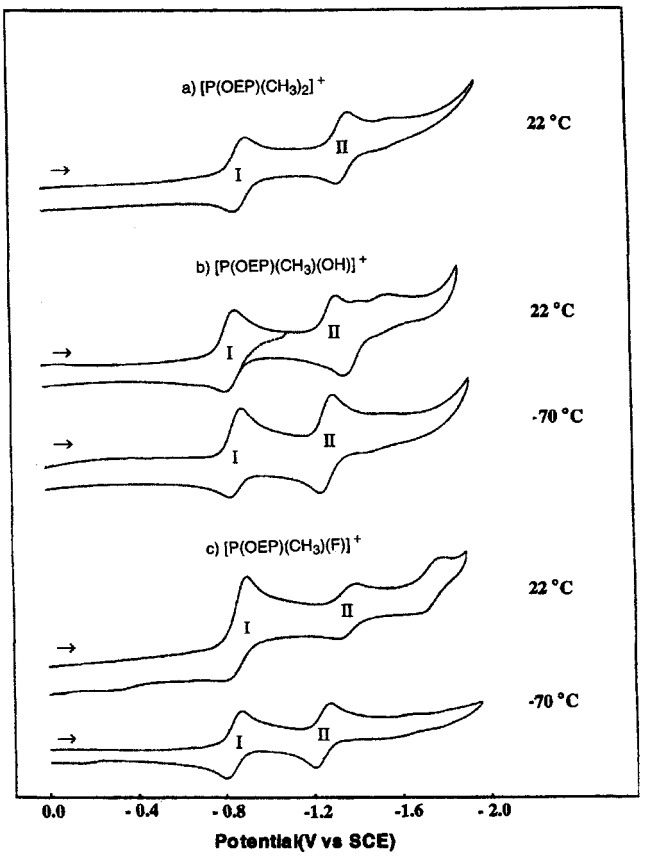

Figure 10. Cyclic voltammograms of (a) $[P(OEP)(CH_3)_2]^+$, (b) $[P(OEP)(CH_3)(OH)]^+$, and (c) $[P(OEP)(CH_3)(F)]^+$ in CH_2Cl_2 containing 0.1 M TBAP.

(99) Barkigia, K. M.; Berber, M. D.; Fajer, J.; Medforth, C. J.; Renner, M. W.; Smith, K. M. *J. Am. Chem. Soc.* **1990**, *112*, 8851.
(100) Sibilia, S. A.; Hu, S.; Piffat, C.; Malamed, D.; Spiro, T. G. *Inorg. Chem.* **1997**, *36*, 1013.
(101) Kadish, K. M.; Van Caemelbecke, E.; D'Souza, F.; Medforth, C. J.; Smith, K. M.; Tabard, A.; Guilard, R. *Inorg. Chem.* **1995**, *34*, 2984.
(102) Sparks, L. D.; Medforth, C. J.; Park, M.-S.; Chamberlain, J. R.; Ondrias, M. R.; Senge, M. O.; Smith, K. M.; Shelnutt, J. A. *J. Am. Chem. Soc.*, **1993**, *115*, 581.
(103) Barkigia, K. M.; Renner, M. W.; Furenlid, L. R.; Medforth, C. J.; Smith, K. M.; Fajer, J. *J. Am. Chem. Soc.*, **1993**, *115*, 3627.

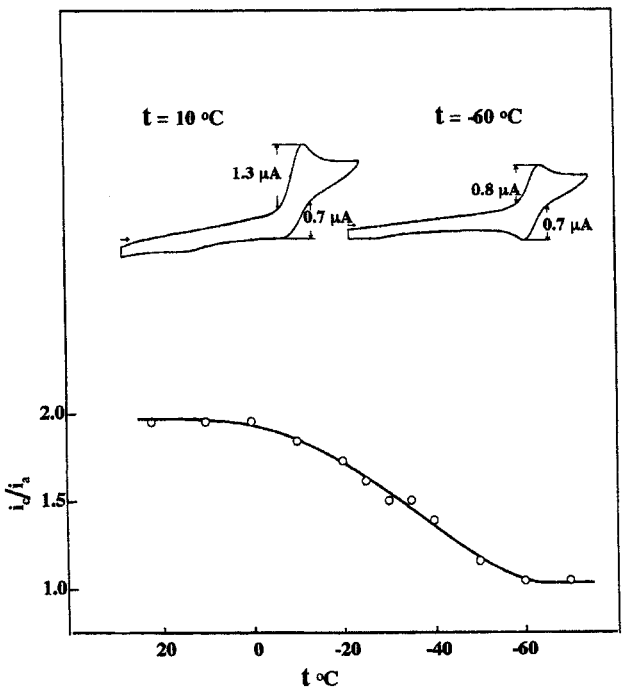

Figure 11. i_c/i_a for first reduction of $[P(OEP)(CH_3)(F)]^+$ in CH_2Cl_2 containing 0.1 M TBAP, monitored as a function of temperature.

potentials for both electrode reactions of each compound are shifted toward more positive values as the electronegativity of the axial ligand increases (see Table 4).

Two major reductions are also seen for the derivatives with X = CH_3, C_2H_5, C_6H_5 and Y = OH. The first reduction is reversible if the scan is reversed at −1.00 V such as in the case of $[P(OEP)(C_2H_5)(OH)]^+$ in Figure 10b. The second reduction of this compound in CH_2Cl_2 is irreversible at room temperature but not at low temperature as shown in Figure 10b. The room-temperature voltammograms of this complex display several small reduction peaks at potentials negative of the cathodic peak II which are attributed to one or more products generated from one or more homogeneous chemical reactions following the second electron transfer. These reactions are slowed at −70 °C and, under these conditions, the second reduction is reversible and located at $E_{1/2}$ = −1.27 V. Similar electrochemical behavior is observed for the other derivatives with a hydroxide axial ligand.

The first reductions of phosphorus porphyrins having X = CH_3 or OCH_3 and Y = F are irreversible at room temperature. The cathodic peak of the first reduction, $E_{pc,}$ is located at −0.77 and −0.80 V for $[P(OEP)(CH_3)(F)]^+$ and $[P(OEP)(OCH_3)(F)]^+$, respectively, in CH_2Cl_2. However, when the temperature is lowered from 22 °C, the ratio of the peak currents i_a and i_c decreases and approaches 1.0 at −60 °C as seen in Figure 10c and Figure 11 for case of $[P(OEP)(CH_3)(F)]^+$. This result suggests an electrochemical EC mechanism for the first reduction at low temperature. A second reversible reduction is observed for $[P(OEP)(CH_3)(F)]^+$ as well as for $[P(OEP)(OCH_3)(F)]^+$ at low temperature which indicates that no chemical reactions occur under these experimantal conditions.

The absolute potential difference between $E_{1/2}$ values for the two reductions of the electrochemically investigated P(V) complexes ranges from 0.45 to 0.57 V depending upon the solvent and the specific set of axial ligands. This separation is similar to $\Delta E_{1/2}$ values reported for previously investigated $[P(TpTP)(OCH_3)_2]^+$, $[Sb(TpTP)(OCH_3)_2]^+$, $[Sb(TPP)(X)(Y)]^+$ and $[Sb(OEP)(X)(Y)]^+$ (where X = CH_3, C_2H_5, C_6H_5 or OCH_3 and Y = CH_3, OH, OCH_3, or F). These porphyrins all undergo electroreductions at the conjugated π ring system of the macrocycle.[16,18,69]

All of the investigtaed phosphorus(V) porphyrins show a single reversible oxidation within the range of the utilized electrochemical solvents. The absolute difference in potential between the first ring-centered oxidation and the first ring-centered reduction of these derivatives varies from 2.19 to 2.36 V in CH_2Cl_2 and these values are within the range of the HOMO−LUMO gap observed for most metalloporphyrins.[104]

Finally it should be noted that the first reduction of the P(V) octaethylporphyrins occurs at potentials more negative than those of the analogous antimony derivatives. For example, $[P(OEP)(CH_3)_2]^+$ and $[P(OEP)(C_2H_5)(OH)]^+$ are reduced at $E_{1/2}$= −0.90 and −0.84 V, respectively, in CH_2Cl_2, while the first reduction of $[Sb(OEP)(CH_3)_2]^+$ and $[Sb(OEP)(C_2H_5)(OH)]^+$ occur at −0.78 and −0.74 V, respectively. This difference of 100−120 mV in potential agrees with results from previous studies on other phosphorus and antimony porphyrins and is due to the stronger inductive (donating) effect of Sb(V) as compared to P(V).[16]

Spectroelectrochemistry. To assign the site of electron transfer, the UV−vis spectra were recorded during thin-layer controlled-potential electroreduction and oxidation of the nine investigated porphyrins in PhCN, 0.2 M TBAP. A summary of the spectral data for these complexes before and after the electron-transfer reaction is given in Table 5 which also lists the potential which was applied in order to carry out each reduction. Examples of the UV−vis spectral changes obtained during the controlled-potential reduction of $[P(OEP)(C_2H_5)(OCH_3)]^+$, $[P(OEP)(CH_3)(OH)]^+$, and $[P(OEP)(OCH_3)(F)]^+$ are presented in the Figure 12.

Similar changes in the electronic absorption spectra were observed upon the two reductions of each compound except for $[P(OEP)(CH_3)(F)]^+$ and $[P(OEP)(OCH_3)(F)]^+$. For example, as the first controlled-potential reduction of $[P(OEP)(C_2H_5)(OCH_3)]^+$ proceeded, the original absorption bands at 421, 551, and 592 nm decreased in intensity and new broad absorption bands appeared at 649 and 790 nm. These spectral changes were reversible, consistent with a ring-centered electron transfer leading to formation of a porphyrin π-anion radical.[105,106]

The second reduction of $[P(OEP)(C_2H_5)(OCH_3)]^+$ led to a further decrease and broadening of the Soret band. New broad bands of low intensity are also seen for the doubly reduced porphyrin at 313, 459, and 567 nm. It has been suggested that an electron transfer between the doubly reduced porphyrin ring and the central phosphorus atom will occur in the case of $[P(OEP)(Cl)_2]^+$ leading to formation of a P(III) porphyrin complex. The same conclusion was obtained for some doubly reduced antimony(V) porphyrins.[16,18,69] P(III) porphyrins, like other porphyrins containing a low valent main group metal exhibit a p-hyper type absorption spectra and is characterized by two absorption bands in the UV region which are located at 350−380 nm and 450−470 nm.[69,107]

In this present study, no Soret bands could be observed for the reduced species at 350−380 nm and this provides no evidence for the formation of P(III) porphyrins upon the second electroreduction. The spectral changes observed when going from the singly to the doubly reduced species are irreversible

(104) Kadish, K. M. *Prog. Inorg. Chem.* **1986**, 34, 435
(105) Felton, R. H. In *The Porphyrins*; Dolphin, D., Ed.; Academic Press: New York, 1979; Vol. IV, pp 53−115.
(106) Kadish, K. M.; Tagliatesta, P.; Hu, Y.; Deng, Y. J.; Mu, X. H.; Bao, L. Y. *Inorg. Chem.* **1991**, *30*, 3737.

Table 5. Spectral Data for P(V) Octaethylporphyrin Complexes and Their Reduction Products in PhCN Containing 0.2 M TBAP

axial ligands		oxidation state	E_{appl}(V)	λ,nm ($10^{-4}\epsilon$)				
CH_3	CH_3	neutral		366(3.3)	430(20.6)[a]	556(1.8)	597(0.9)	
	OCH_3^-			362(1.6)	420(17.6)	550(0.8)	591(0.7)	
	OH^-			356(1.9)	419(19.8)	547(1.0)	590(1.1)	
	F^-			364(1.3)	416(22.8)	549(0.6)	591(0.9)	
C_2H_5	OCH_3^-			358(1.8)	421(19.5)	551(0.6)	592(0.6)	
	OH^-			356(2.2)	420(20.5)	549(1.2)	590(0.9)	
C_6H_5	OCH_3^-			357(1.5)	420(21.3)	552(0.6)	595(0.9)	
	OH^-			357(2.0)	419(23.4)	550(1.2)	593(1.5)	
OCH_3	F^-			337(0.6)	407(18.5)	545(0.5)	589(1.2)	
CH_3	CH_3	singly	−1.00	365(2.5)	431(9.8)		685(0.6)	
	OCH_3^-	reduced	−1.00	361(1.8)	420(6.7)		647(0.8)	
	OH^-		−1.00	363(1.9)	420(6.4)		641(0.8)	794(0.2)
	F^-		−0.90	311(1.2)	415(3.6)	481(3.1)	644(0.5)	799(0.6)
C_2H_5	OCH_3^-		−1.00	360(2.1)	422(7.6)		649(0.9)	
	OH^-		−1.00	348(2.1)	419(10.6)		643(0.4)[b]	
C_6H_5	OCH_3^-		−1.00	363(2.2)	420(8.7)		651(1.0)	
	OH^-		−1.00	354(2.0)	420(9.5)	483(1.4)	647(0.6)[c]	
OCH_3	F^-		−0.80	309(1.1)	406(3.6)	475(3.0)		786(0.6)
CH_3	CH_3	doubly	−1.40	312(1.9)	430(2.7)	463(2.9)	569(1.0)	
	OCH_3^-	reduced	−1.40	311(0.6)	413(1.2)	458(0.8)	564(0.3)	
	OH^-		−1.30	306(1.3)	417(2.7)	459(3.8)	538(0.4)	811(1.0)
	F^-		−1.30	307(1.6)	404(3.1)	457(3.1)	557(0.7)	
C_2H_5	OCH_3^-		−1.40	313(1.6)	416(3.8)	459(1.9)	567(0.8)	
	OH^-		−1.30	348(1.7)	418(7.9)	463(2.3)	538(0.8)	812(0.5)
C_6H_5	OCH_3^-		−1.40	304(1.7)	406(3.5)	464(2.8)	561(0.8)	
	OH^-		−1.40	306(1.4)	397(2.2)	463(5.6)	550(0.5)	800(1.4)
OCH_3	F^-		−1.35	308(1.1)	398(2.8)	475(2.5)	552(0.7)	
CH_3	OH^-	triply	−1.60	364(1.7)		454(2.3)	585(0.6)	751(2.1)
	F^-	reduced	−1.60	332(1.6)	406(2.8)	447(1.6)	581(0.7)	739(1.4)
C_2H_5	OH^-		−1.50	308(1.3)		463(4.1)	585(0.2)	754(0.9)
C_6H_5	OH^-		−1.60	367(2.0)		455(2.8)	587(0.8)	742(2.4)
OCH_3	F^-		−1.60	332(1.7)	397(3.2)	441(1.3)	560(0.8)	728(0.9)

[a−c] Additional absorption peaks are seen at λ, nm($10^{-4}\epsilon$): [a] 408(4.5). [b] 538(0.9), 571(0.7). [c] 545(0.8), 579(0.7).

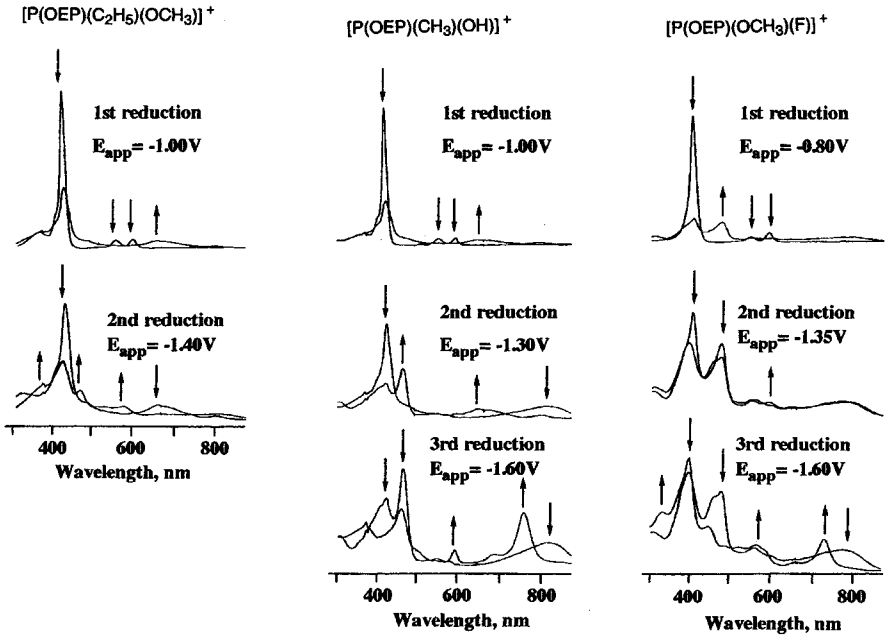

Figure 12. Thin-layer spectral changes during reductions of $[P(OEP)(C_2H_5)(OCH_3)]^+$, $[P(OEP)(CH_3)(OH)]^+$, and $[P(OEP)(OCH_3)(F)]^+$ in PhCN containing 0.2 M TBAP.

but is very similar to that of the original compound showing only a small decrease in intensity. The UV−vis spectrum of the neutral species can be recovered when the controlled potential is set back to 0.0 V. These results suggest that the main reduction product is a porphyrin dianion although some chemical reactions may occur after the second electroreduction.

Similar spectral changes are observed during the two controlled-potential reductions of $[P(OEP)(CH_3)(F)]^+$ and $[P(OEP)(OCH_3)(F)]^+$. The initial Soret band at 416 nm for $[P(OEP)(CH_3)(F)]^+$ and at 406 nm for $[P(OEP)(OCH_3)(F)]^+$ decreases in intensity as the first reduction proceeds and a new broad absorption band appears at around 790 nm which is characteristic of a ring-centered electroreduction. However, an additional broad band also appears at 455−475 nm which indicates that a chemical reaction has occurred after the first electroreduction. The spectra of the recovered species after reoxidation is again similar to the neutral compound but shows a decrease in intensity. At the same time, the new band at 455−475 nm can still be observed in the reoxidized species. The results agree with the electro-

(107) Sayer, P.; Gouterman, M.; Connell, C. R. *J. Am. Chem. Soc.* **1977**, *99*, 1082.

Table 6. ESR Parameters for the One-Electron-Reduced Products of the Phosphorus(V) Porphyrins in CH_2Cl_2 Containing 0.2 M TBAP

axial ligands		T = 295 K		T = 115 K	
		g	ΔHpp(*G*)	*g*	ΔHpp(*G*)
C_6H_5	OCH_3^-	2.001(6)	5.61	2.002(9)	2.15
C_2H_5	OCH_3^-	2.007(1)	6.78	2.003(4)	2.69
CH_3	OCH_3^-	2.005(3)	7.54	2.004(3)	4.31
C_6H_5	OH^-	2.006(5)	5.39	2.003(4)	8.08
C_2H_5	OH^-	2.006(1)	5.92	2.004(2)	7.54
CH_3	OH^-	2.001(4)	5.92	2.000(1)	8.62
CH_3	CH_3	2.000(5)	5.39	2.002(1)	1.94
CH_3	F^-	2.009(3)	6.46	2.003(8)	6.46
OCH_3^-	F^-	2.000(3)	8.08	1.998(9)	6.68

chemistry and suggests that the first reduction is not reversible. Further controlled-potential reduction at potential negative of the second reduction leads to a species with a further reduced Soret band (see Figure 12) and this result is consistent with formation of a porphyrin dianion.

ESR Characterization. The singly reduced products of each investigated phosphorus porphyrin have isotropic ESR signals and *g* values which range from 1.998 to 2.004 at 115 K and from 2.000 to 2.007 at 295 K. The results are consistent with formation of a porphyrin π-anion radical as the main product of the first electroreduction. The spectral line widths, ΔH, range from 1.94 to 6.68 G at 115 K for all of the complexes except for those containing a coordinated OH^- axial ligand. These ΔH values increase with temperature and vary from 5.39 to 8.08 G at 295 K (see Table 6). This result agrees with previous reports in the literature and suggests an interaction between the unpaired electron on the porphyrin macrocycle and the central phosphorus nucleus.[18]

The phosphorus porphyrins with one OH^- axial ligand have ΔH values which are in the same range as for the other complexes at 295 K. However, this is not the case at low temperature (115 K) where the ΔH values of those porphyrins are higher than values for the other examined derivatives in this study. It should be also noted that the ΔH values obtained at 115 K are smaller than those obtained at 295 K (see Table 6). To our knowledge this has not previously been observed for metalloporphyrins and might indicate a chemical exchange between the radicals which can exist in two distinct forms.[108]

The singly reduced porphyrins are stable and no ESR signals can be observed after reoxidation by bulk electrolysis at 0.0 V. The doubly reduced porphyrins are ESR silent, suggested that the second reduction occurs at the conjugated π ring system of the macrocycle.

Acknowledgment. Part of this work was supported by a Grant-in-Aid for Scientific Research (Nos. 09239103, 09440218, 11166248, 11304044) from the Ministry of Education, Science, Sports, and Culture, Japan (K.A.), and the Robert A. Welch Foundation (K.M.K., Grant E-680).

Supporting Information Available: Positional and thermal parameters and interatomic distances and angles for **1**-PF_6, **2b**-ClO_4, **2c**-PF_6, **2d**-ClO_4, **3b**, **6f**-ClO_4, **7a**-ClO_4, **9a**-PF_6, **9c**-PF_6, **11a**-PF_6, and **11b**-PF_6; ORTEP drawings of **1**-PF_6, **2c**-PF_6, **7a**-ClO_4, and **9a**-PF_6; figures of the deviations (in units of 0.01 Å) of the skeletal atoms from the mean plane defined by the 24 core atoms of the porphyrin for **1**-PF_6, **2c**-PF_6, **2d**-ClO_4, **6f**-ClO_4, **7a**-ClO_4, **9a**-PF_6, **9c**-PF_6, **11a**-PF_6, and **11b**-PF_6. This material is available free of charge via the Internet at http://pubs.acs.org.

IC010595E

(108) Wertz, J. E.; Bolton, J. R. *Electron Spin Resonance, Elementary Theory and Practical Applications*; Chapman and Hall: New York, 1986; pp 192−222.